

**Yim-Shu Lee and Martin
H. L. Chow**

*Department of Electronic and
Information Engineering,
The Hong Kong Polytechnic,
University Hung Hom,
Hong Kong*

10.1 Introduction	145
10.2 Single-phase Diode Rectifiers	145
10.2.1 Single-phase Half-wave Rectifiers • 10.2.2 Single-phase Full-wave Rectifiers • 10.2.3 Performance Parameters • 10.2.4 Design Considerations	
10.3 Three-phase Diode Rectifiers	150
10.3.1 Three-phase Star Rectifiers • 10.3.2 Three-phase Bridge Rectifiers • 10.3.3 Operation of Rectifiers with Finite Source Inductance	
10.4 Poly-phase Diode Rectifiers	155
10.4.1 Six-phase Star Rectifier • 10.4.2 Six-phase Series Bridge Rectifier • 10.4.3 Six-phase Parallel Bridge Rectifier	
10.5 Filtering Systems in Rectifier Circuits	158
10.5.1 Inductive-input DC Filters • 10.5.2 Capacitive-input DC Filters	
10.6 High-frequency Diode Rectifier Circuits.....	162
10.6.1 Forward Rectifier Diode, Flywheel Diode, and Magnetic-reset Clamping Diode in a Forward Converter • 10.6.2 Flyback Rectifier Diode and Clamping Diode in a Flyback Converter • 10.6.3 Design Considerations • 10.6.4 Precautions in Interpreting Simulation Results	
Further Reading	177

10.1 Introduction

This chapter describes the application and design of diode rectifier circuits. It covers single-phase rectifier circuits, three-phase rectifier circuits, poly-phase rectifier circuits, and high-frequency rectifier circuits. The objectives of this chapter are:

- To enable the readers to understand the operation of typical rectifier circuits.
- To enable the readers to appreciate the different qualities of rectifiers required for different applications.
- To enable the reader to design practical rectifier circuits.

The high-frequency rectifier waveforms given are obtained from PSPICE simulations, which take into account the secondary effects of stray and parasitic components. In this way, the waveforms can closely resemble the real ones. These waveforms are particularly useful to help designers determine the practical voltage, current, and other ratings of high-frequency rectifiers.

10.2 Single-phase Diode Rectifiers

There are two types of single-phase diode rectifier that convert a single-phase ac supply into a dc voltage, namely, single-phase half-wave rectifiers and single-phase full-wave rectifiers. In the following subsections, the operations of these rectifier circuits are examined and their performances are analyzed and compared in a tabulated form. For the sake of simplicity, the diodes are considered to be ideal, i.e. they have zero forward voltage drop and reverse recovery time. This assumption is generally valid for the case of diode rectifiers which use the mains, a low-frequency source, as the input, and when the forward voltage drop is small compared with the peak voltage of the mains. Furthermore, it is assumed that the load is purely resistive such that the load voltage and the load current have similar waveforms. In Section 10.5, Filtering Systems in Rectifiers, the effects of inductive load and capacitive load on a diode rectifier are considered in detail.

10.2.1 Single-phase Half-wave Rectifiers

The simplest single-phase diode rectifier is the single-phase half-wave rectifier. A single-phase half-wave rectifier with resistive load is shown in Fig. 10.1. The circuit consists of only one diode that is usually fed with a secondary transformer as shown. During the positive half-cycle of the transformer secondary voltage, diode D conducts. During the negative half-cycle, diode D stops conducting. Assuming that the transformer has zero internal impedance and provides perfect sinusoidal voltage on its secondary winding, the voltage and current waveforms of resistive load R and the voltage waveform of diode D are shown in Fig. 10.2.

By observing the voltage waveform of diode D in Fig. 10.2, it is clear that the peak inverse voltage (PIV) of diode D is equal to V_m during the negative half-cycle of the transformer secondary voltage. Hence the peak repetitive reverse voltage (V_{RRM}) rating of diode D must be chosen to be higher than V_m to avoid reverse breakdown. In the positive half-cycle of the transformer secondary voltage, diode D has a forward current which is equal to the load current, therefore the peak repetitive forward current (I_{FRM}) rating of diode D must be chosen to

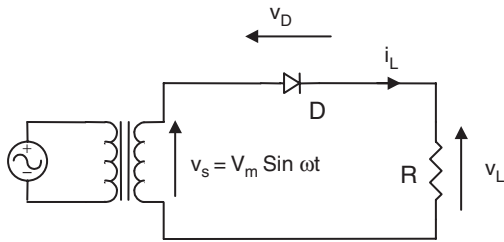


FIGURE 10.1 A single-phase half-wave rectifier with resistive load.

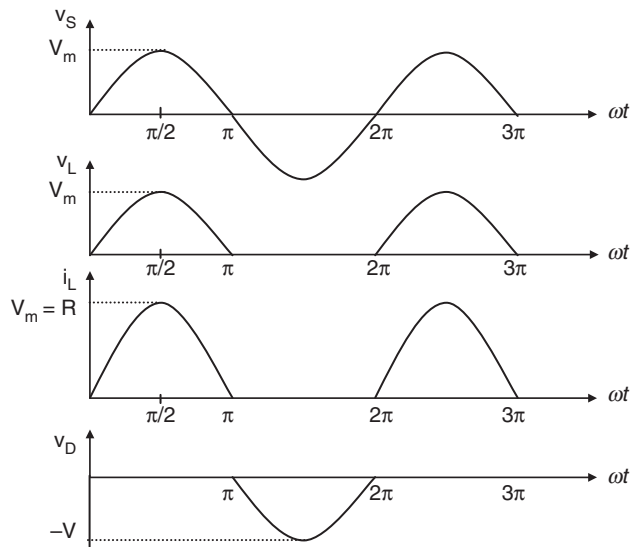


FIGURE 10.2 Voltage and current waveforms of the half-wave rectifier with resistive load.

be higher than the peak load current, $V_m = R$, in practice. In addition, the transformer has to carry a dc current that may result in a dc saturation problem of the transformer core.

10.2.2 Single-phase Full-wave Rectifiers

There are two types of single-phase full-wave rectifier, namely, full-wave rectifiers with center-tapped transformer and bridge rectifiers. A full-wave rectifier with a center-tapped transformer is shown in Fig. 10.3. It is clear that each diode, together with the associated half of the transformer, acts as a half-wave rectifier. The outputs of the two half-wave rectifiers are combined to produce full-wave rectification in the load. As far as the transformer is concerned, the dc currents of the two half-wave rectifiers are equal and opposite, such that there is no dc current for creating a transformer core saturation problem. The voltage and current waveforms of the full-wave rectifier are shown in Fig. 10.4. By observing diode voltage waveforms v_{D1} and v_{D2} in Fig. 10.4, it is clear that the PIV of the diodes is equal to $2V_m$ during their blocking state. Hence the V_{RRM} rating of the diodes must be chosen to be higher than $2V_m$ to avoid reverse breakdown. (Note that, compared with the half-wave rectifier shown in Fig. 10.1, the full-wave rectifier has twice the dc output voltage, as shown in Section 10.2.4.) During its conducting state, each diode has a forward current which is equal to the load current, therefore the I_{FRM} rating of these diodes must be chosen to be higher than the peak load current, $V_m = R$, in practice.

Employing four diodes instead of two, a bridge rectifier as shown in Fig. 10.5 can provide full-wave rectification without using a center-tapped transformer. During the positive half-cycle of the transformer secondary voltage, the current flows to the load through diodes D_1 and D_2 . During the negative half-cycle, D_3 and D_4 conduct. The voltage and current waveforms of the bridge rectifier are shown in Fig. 10.6 As with the full-wave rectifier with center-tapped transformer, the I_{FRM} rating of the employed diodes must be chosen to be higher than the peak load current, $V_m = R$. However, the PIV of the diodes is reduced from $2V_m$ to V_m during their blocking state.

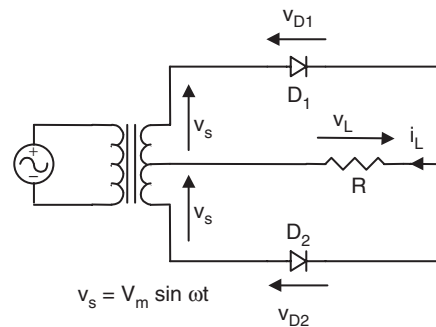


FIGURE 10.3 Full-wave rectifier with center-tapped transformer.

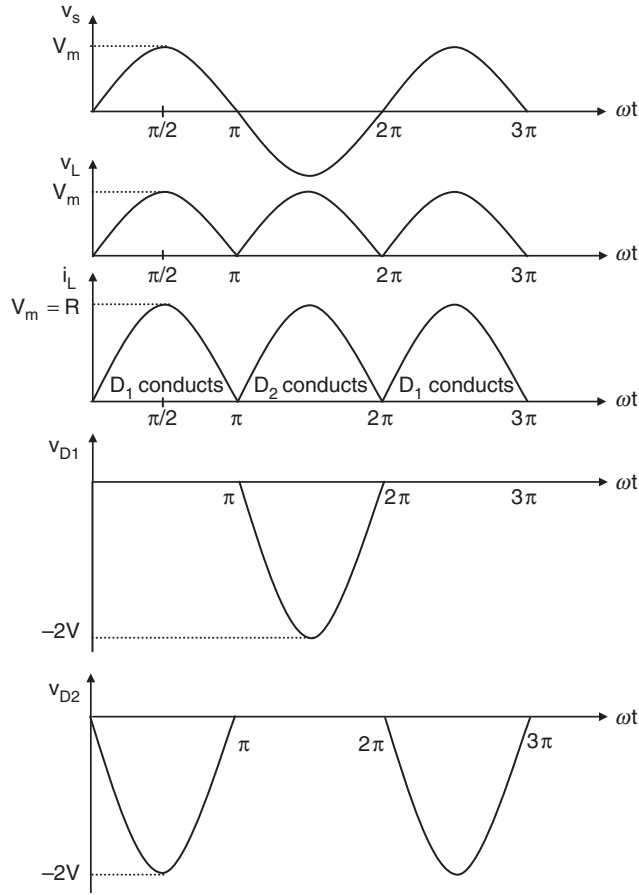


FIGURE 10.4 Voltage and current waveforms of the full-wave rectifier with center-tapped transformer.

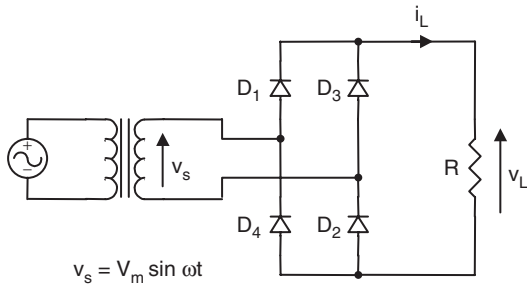


FIGURE 10.5 Bridge rectifier.

10.2.3 Performance Parameters

In this subsection, the performance of the rectifiers mentioned above will be evaluated in terms of the following parameters.

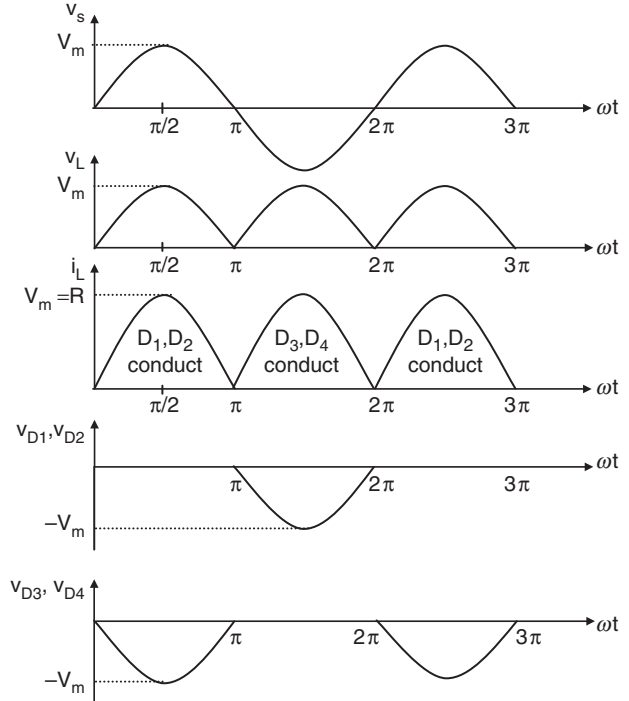


FIGURE 10.6 Voltage and current waveforms of the bridge rectifier.

10.2.3.1 Voltage Relationships

The average value of the load voltage v_L is V_{dc} and it is defined as

$$V_{dc} = \frac{1}{T} \int_0^T v_L(t) dt \quad (10.1)$$

In the case of a half-wave rectifier, Fig. 10.2 indicates that load voltage $v_L(t) = 0$ for the negative half-cycle. Note that the angular frequency of the source $\omega = 2\pi/T$, and Eq. (10.1) can be re-written as

$$V_{dc} = \frac{1}{2\pi} \int_0^\pi V_m \sin \omega t d(\omega t) \quad (10.2)$$

Therefore,

$$\text{Half-wave } V_{dc} = \frac{V_m}{\pi} = 0.318 V_m \quad (10.3)$$

In the case of a full-wave rectifier, Figs. 10.4 and 10.6 indicate that $v_L(t) = V_m |\sin \omega t|$ for both the positive and negative half-cycles. Hence Eq. (10.1) can be re-written as

$$V_{dc} = \frac{1}{\pi} \int_0^\pi V_m \sin \omega t d(\omega t) \quad (10.4)$$

Therefore,

$$\text{Full-wave } V_{dc} = \frac{2V_m}{\pi} = 0.636 V_m \quad (10.5)$$

The root-mean-square (rms) value of load voltage v_L is V_L , which is defined as

$$V_L = \left[\frac{1}{T} \int_0^T v_L^2(t) dt \right]^{1/2} \quad (10.6)$$

In the case of a half-wave rectifier, $v_L(t) = 0$ for the negative half-cycle, therefore Eq. (10.6) can be re-written as

$$V_L = \sqrt{\frac{1}{2\pi} \int_0^\pi (V_m \sin \omega t)^2 d(\omega t)} \quad (10.7)$$

or

$$\text{Half-wave } V_L = \frac{V_m}{2} = 0.5 V_m \quad (10.8)$$

In the case of a full-wave rectifier, $v_L(t) = V_m |\sin \omega t|$ for both the positive and negative half-cycles. Hence Eq. (10.6) can be re-written as

$$V_L = \sqrt{\frac{1}{\pi} \int_0^\pi (V_m \sin \omega t)^2 d(\omega t)} \quad (10.9)$$

or

$$\text{Full-wave } V_L = \frac{V_m}{\sqrt{2}} = 0.707 V_m \quad (10.10)$$

The result of Eq. (10.10) is as expected because the rms value of a full-wave rectified voltage should be equal to that of the original ac voltage.

10.2.3.2 Current Relationships

The average value of load current i_L is I_{dc} and because load R is purely resistive it can be found as

$$I_{dc} = \frac{V_{dc}}{R} \quad (10.11)$$

The rms value of load current i_L is I_L and it can be found as

$$I_L = \frac{V_L}{R} \quad (10.12)$$

In the case of a half-wave rectifier, from Eq. (10.3)

$$\text{Half-wave } I_{dc} = \frac{0.318 V_m}{R} \quad (10.13)$$

and from Eq. (10.8)

$$\text{Half-wave } I_L = \frac{0.5 V_m}{R} \quad (10.14)$$

In the case of a full-wave rectifier, from Eq. (10.5)

$$\text{Full-wave } I_{dc} = \frac{0.636 V_m}{R} \quad (10.15)$$

and from Eq. (10.10)

$$\text{Full-wave } I_L = \frac{0.707 V_m}{R} \quad (10.16)$$

10.2.3.3 Rectification Ratio

The rectification ratio, which is a figure of merit for comparing the effectiveness of rectification, is defined as

$$\sigma = \frac{P_{dc}}{P_L} = \frac{V_{dc} I_{dc}}{V_L I_L} \quad (10.17)$$

In the case of a half-wave diode rectifier, the rectification ratio can be determined by substituting Eqs. (10.3), (10.13), (10.8), and (10.14) into Eq. (10.17).

$$\text{Half-wave } \sigma = \frac{(0.318 V_m)^2}{(0.5 V_m)^2} = 40.5\% \quad (10.18)$$

In the case of a full-wave rectifier, the rectification ratio is obtained by substituting Eqs. (10.5), (10.15), (10.10), and (10.16) into Eq. (10.17).

$$\text{Full-wave } \sigma = \frac{(0.636 V_m)^2}{(0.707 V_m)^2} = 81\% \quad (10.19)$$

10.2.3.4 Form Factor

The form factor (FF) is defined as the ratio of the root-mean-square value (heating component) of a voltage or current to its average value,

$$\text{FF} = \frac{V_L}{V_{dc}} \quad \text{or} \quad \frac{I_L}{I_{dc}} \quad (10.20)$$

In the case of a half-wave rectifier, the FF can be found by substituting Eqs. (10.8) and (10.3) into Eq. (10.20).

$$\text{Half-wave } \text{FF} = \frac{0.5 V_m}{0.318 V_m} = 1.57 \quad (10.21)$$

In the case of a full-wave rectifier, the FF can be found by substituting Eqs. (10.16) and (10.15) into Eq. (10.20).

$$\text{Full-wave } \text{FF} = \frac{0.707 V_m}{0.636 V_m} = 1.11 \quad (10.22)$$

10.2.3.5 Ripple Factor

The ripple factor (RF), which is a measure of the ripple content, is defined as

$$\text{RF} = \frac{V_{ac}}{V_{dc}} \quad (10.23)$$

where V_{ac} is the effective (rms) value of the ac component of load voltage v_L .

$$V_{ac} = \sqrt{V_L^2 - V_{dc}^2} \quad (10.24)$$

Substituting Eq. (10.24) into Eq. (10.23), the RF can be expressed as

$$\text{RF} = \sqrt{\left(\frac{V_L}{V_{dc}}\right)^2 - 1} = \sqrt{\text{FF}^2 - 1} \quad (10.25)$$

In the case of a half-wave rectifier,

$$\text{Half-wave RF} = \sqrt{1.57^2 - 1} = 1.21 \quad (10.26)$$

In the case of a full-wave rectifier,

$$\text{Full-wave RF} = \sqrt{1.11^2 - 1} = 0.482 \quad (10.27)$$

10.2.3.6 Transformer Utilization Factor

The transformer utilization factor (TUF), which is a measure of the merit of a rectifier circuit, is defined as the ratio of the dc output power to the transformer volt-ampere (VA) rating required by the secondary winding,

$$\text{TUF} = \frac{P_{dc}}{V_s I_s} = \frac{V_{dc} I_{dc}}{V_s I_s} \quad (10.28)$$

where V_s and I_s are the rms voltage and rms current ratings of the secondary transformer.

$$V_s = \frac{V_m}{\sqrt{2}} = 0.707 V_m \quad (10.29)$$

The rms value of the transformer secondary current I_s is the same as that of the load current I_L . For a half-wave rectifier, I_s can be found from Eq. (10.14).

$$\text{Half-wave } I_s = \frac{0.5 V_m}{R} \quad (10.30)$$

For a full-wave rectifier, I_s is found from Eq. (10.16).

$$\text{Full-wave } I_s = \frac{0.707 V_m}{R} \quad (10.31)$$

Therefore, the TUF of a half-wave rectifier can be obtained by substituting Eqs. (10.3), (10.13), (10.29), and (10.30) into Eq. (10.28).

$$\text{Half-wave TUF} = \frac{0.318^2}{0.707 \times 0.5} = 0.286 \quad (10.32)$$

The poor TUF of a half-wave rectifier signifies that the transformer employed must have a 3.496 (1/0.286) VA rating in order to deliver 1 W dc output power to the load. In addition, the transformer secondary winding has to carry a dc current that may cause magnetic core saturation. As a result, half-wave rectifiers are used only when the current requirement is small.

In the case of a full-wave rectifier with center-tapped transformer, the circuit can be treated as two half-wave rectifiers operating together. Therefore, the transformer secondary VA rating, $V_s I_s$, is double that of a half-wave rectifier, but the output dc power is increased by a factor of four due to higher the rectification ratio as indicated by Eqs. (10.5) and (10.15). Therefore, the TUF of a full-wave rectifier with center-tapped transformer can be found from Eq. (10.32)

$$\text{Full-wave TUF} = \frac{4 \times 0.318^2}{2 \times 0.707 \times 0.5} = 0.572 \quad (10.33)$$

In the case of a bridge rectifier, it has the highest TUF in single-phase rectifier circuits because the currents flowing in both the primary and secondary windings are continuous sinewaves. By substituting Eqs. (10.5), (10.15), (10.29), and (10.31) into Eq. (10.28), the TUF of a bridge rectifier can be found.

$$\text{Bridge TUF} = \frac{0.636^2}{(0.707)^2} = 0.81 \quad (10.34)$$

The transformer primary VA rating of a full-wave rectifier is equal to that of a bridge rectifier since the current flowing in the primary winding is also a continuous sinewave.

10.2.3.7 Harmonics

Full-wave rectifier circuits with resistive load do not produce harmonic currents in their transformers. In half-wave rectifiers, harmonic currents are generated. The amplitudes of the harmonic currents of a half-wave rectifier with resistive load, relative to the fundamental, are given in Table 10.1. The extra loss caused by the harmonics in the resistive loaded rectifier circuits is often neglected because it is not high compared with other losses. However, with non-linear loads, harmonics can cause appreciable loss and other problems such as poor power factor and interference.

TABLE 10.1 Harmonic percentages of a half-wave rectifier with resistive load

Harmonic	2nd	3rd	4th	5th	6th	7th	8th
%	21.2	0	4.2	0	1.8	0	1.01

10.2.4 Design Considerations

In a practical design, the goal is to achieve a given dc output voltage. Therefore, it is more convenient to put all the design parameters in terms of V_{dc} . For example, the rating and turns ratio of the transformer in a rectifier circuit can be easily determined if the rms input voltage to the rectifier is in terms of the required output voltage V_{dc} .

Denote the rms value of the input voltage to the rectifier as V_s , which is equal to $0.707V_m$. Based on this relation and Eq. (10.3), the rms input voltage to a half-wave rectifier is found as

$$\text{Half-wave } V_s = 2.22V_{dc} \quad (10.35)$$

Similarly, from Eqs. (10.5) and (10.29), the rms input voltage per secondary winding of a full-wave rectifier is found as

$$\text{Full-wave } V_s = 1.11V_{dc} \quad (10.36)$$

Another important design parameter is the V_{RRM} rating of the diodes employed.

In the case of a half-wave rectifier, from Eq. (10.3),

$$\text{Half-wave } V_{RRM} = V_m = \frac{V_{dc}}{0.318} = 3.14V_{dc} \quad (10.37)$$

In the case of a full-wave rectifier with center-tapped transformer, from Eq. (10.5),

$$\text{Full-wave } V_{RRM} = 2V_m = \frac{2V_{dc}}{0.636} = 3.14V_{dc} \quad (10.38)$$

In the case of a bridge rectifier, also from Eq. (10.5),

$$\text{Bridge } V_{RRM} = V_m = \frac{V_{dc}}{0.636} = 1.57V_{dc} \quad (10.39)$$

It is important to evaluate the I_{FRM} rating of the employed diodes in rectifier circuits.

In the case of a half-wave rectifier, from Eq. (10.13),

$$\text{Half-wave } I_{FRM} = \frac{V_m}{R} = \frac{I_{dc}}{0.318} = 3.14I_{dc} \quad (10.40)$$

In the case of full-wave rectifiers, from Eq. (10.15),

$$\text{Full-wave } I_{FRM} = \frac{V_m}{R} = \frac{I_{dc}}{0.636} = 1.57I_{dc} \quad (10.41)$$

The important design parameters of basic single-phase rectifier circuits with resistive loads are summarized in Table 10.2.

10.3 Three-phase Diode Rectifiers

It has been shown in Section 10.2 that single-phase diode rectifiers require a rather high transformer VA rating for a given dc output power. Therefore, these rectifiers are suitable only for low to medium power applications. For power output higher than 15 kW, three-phase or poly-phase diode rectifiers should be employed. There are two types of three-phase diode rectifier that convert a three-phase ac supply into a dc voltage, namely, star rectifiers and bridge rectifiers. In the following subsections,

TABLE 10.2 Important design parameters of basic single-phase rectifier circuits with resistive load

	Half-wave rectifier	Full-wave rectifier with center-tapped transformer	Full-wave bridge rectifier
Peak repetitive reverse voltage V_{RRM}	$3.14V_{dc}$	$3.14V_{dc}$	$1.57V_{dc}$
RMS input voltage per transformer leg V_s	$2.22V_{dc}$	$1.11V_{dc}$	$1.11V_{dc}$
Diode average current $I_{F(AV)}$	$1.00I_{dc}$	$0.50I_{dc}$	$0.50I_{dc}$
Peak repetitive forward current I_{FRM}	$3.14I_{F(AV)}$	$1.57I_{F(AV)}$	$1.57I_{F(AV)}$
Diode rms current $I_{F(RMS)}$	$1.57I_{dc}$	$0.785I_{dc}$	$0.785I_{dc}$
Form factor of diode current $I_{F(RMS)}/I_{F(AV)}$	1.57	1.57	1.57
Rectification ratio	0.405	0.81	0.81
Form factor	1.57	1.11	1.11
Ripple factor	1.21	0.482	0.482
Transformer rating primary VA	$2.69P_{dc}$	$1.23P_{dc}$	$1.23P_{dc}$
Transformer rating secondary VA	$3.49P_{dc}$	$1.75P_{dc}$	$1.23P_{dc}$
Output ripple frequency f_r	$1f_i$	$2f_i$	$2f_i$

the operations of these rectifiers are examined and their performances are analyzed and compared in tabulated form. For the sake of simplicity, the diodes and the transformers are considered to be ideal, i.e. the diodes have zero forward voltage drop and reverse current, and the transformers possess no resistance and no leakage inductance. Furthermore, it is assumed that the load is purely resistive, such that the load voltage and the load current have similar waveforms. In Section 10.5 Filtering Systems in Rectifier Circuits, the effects of inductive load and capacitive load on a diode rectifier are considered in detail.

10.3.1 Three-phase Star Rectifiers

10.3.1.1 Basic Three-phase Star Rectifier Circuit

A basic three-phase star rectifier circuit is shown in Fig. 10.7. This circuit can be considered as three single-phase half-wave rectifiers combined together. Therefore it is sometimes referred to as a three-phase half-wave rectifier. The diode in a particular phase conducts during the period when the voltage on that phase is higher than that on the other two phases. The voltage waveforms of each phase and the load are shown in Fig. 10.8. It is clear that, unlike the single-phase rectifier circuit, the conduction angle of each diode is $2\pi/3$, instead of π . This circuit finds uses where the required dc output voltage is relatively low and the required output current is too large for a practical single-phase system.

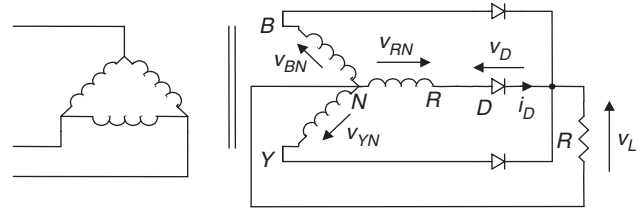


FIGURE 10.7 Three-phase star rectifier.

Taking phase R as an example, diode D conducts from $\pi/6$ to $5\pi/6$. Therefore, using Eq. (10.1) the average value of the output can be found as

$$V_{dc} = \frac{3}{2\pi} \int_{\pi/6}^{5\pi/6} V_m \sin \theta d\theta \quad (10.42)$$

or

$$V_{dc} = V_m \frac{3}{\pi} \frac{\sqrt{3}}{2} = 0.827 V_m \quad (10.43)$$

Similarly, using Eq. (10.6), the rms value of the output voltage can be found as

$$V_L = \sqrt{\frac{3}{2\pi} \int_{\pi/6}^{5\pi/6} (V_m \sin \theta)^2 d\theta} \quad (10.44)$$

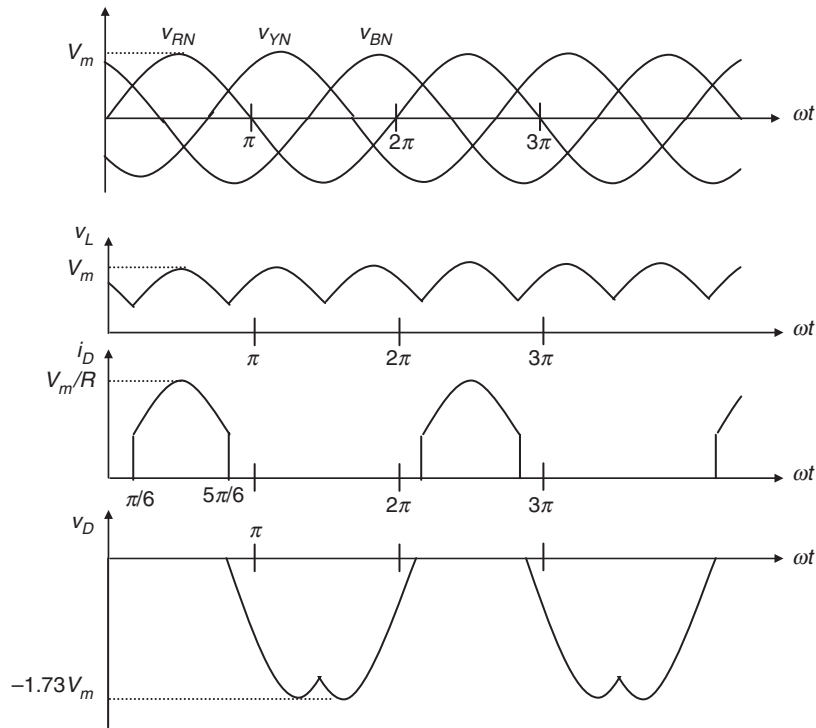


FIGURE 10.8 Waveforms of voltage and current of the three-phase star rectifier shown in Fig. 10.7.

TABLE 10.3 Important design parameters of the three-phase rectifier circuits with the resistive load

	Three-phase star rectifier	Three-phase double-star rectifier with inter-phase transformer	Three-phase bridge rectifier
Peak repetitive reverse voltage V_{RRM}	$2.092V_{dc}$	$1.06V_{dc}$	$1.05V_{dc}$
RMS input voltage per transformer leg V_s	$0.855V_{dc}$	$0.855V_{dc}$	$0.428V_{dc}$
Diode average current $I_{F(AV)}$	$0.333I_{dc}$	$0.167I_{dc}$	$0.333I_{dc}$
Peak repetitive forward current I_{FRM}	$3.63I_{F(AV)}$	$3.15I_{F(AV)}$	$3.14I_{F(AV)}$
Diode rms current $I_{F(RMS)}$	$0.587I_{dc}$	$0.293I_{dc}$	$0.579I_{dc}$
Form factor of diode current $I_{F(RMS)}/I_{F(AV)}$	1.76	1.76	1.74
Rectification ratio	0.968	0.998	0.998
Form factor	1.0165	1.0009	1.0009
Ripple factor	0.182	0.042	0.042
Transformer rating primary VA	$1.23P_{dc}$	$1.06P_{dc}$	$1.05P_{dc}$
Transformer rating secondary VA	$1.51P_{dc}$	$1.49P_{dc}$	$1.05P_{dc}$
Output ripple frequency f_r	$3f_i$	$6f_i$	$6f_i$

or

$$V_L = V_m \sqrt{\frac{3}{2\pi} \left(\frac{\pi}{3} + \frac{\sqrt{3}}{4} \right)} = 0.84V_m \quad (10.45)$$

In addition, the rms current in each transformer secondary winding can also be found as

$$I_s = I_m \sqrt{\frac{1}{2\pi} \left(\frac{\pi}{3} + \frac{\sqrt{3}}{4} \right)} = 0.485I_m \quad (10.46)$$

where $I_m = V_m/R$.

Based on the relationships stated in Eqs. (10.43), (10.45), and (10.46), all the important design parameters of the three-phase star rectifier can be evaluated, as listed in Table 10.3, which is given at the end of Subsection 10.3.2. Note that, as with a single-phase half-wave rectifier, the three-phase star rectifier shown in Fig. 10.7 has direct currents in the secondary windings that can cause a transformer core saturation problem. In addition, the currents in the primary do not sum

to zero. Therefore it is preferable not to have star-connected primary windings.

10.3.1.2 Three-phase Inter-star Rectifier Circuit

The transformer core saturation problem in the three-phase star rectifier can be avoided by a special arrangement in its secondary windings, known as zig-zag connection. The modified circuit is called the three-phase inter-star or zig-zag rectifier circuit, as shown in Fig. 10.9. Each secondary phase voltage is obtained from two equal-voltage secondary windings (with a phase displacement of $\pi/3$) connected in series so that the dc magnetizing forces due to the two secondary windings on any limb are equal and opposite. At the expense of extra secondary windings (increasing the transformer secondary rating factor from 1.51 to 1.74 VA/W), this circuit connection eliminates the effects of core saturation and reduces the transformer primary rating factor to the minimum of 1.05 VA/W. Apart from transformer ratings, all the design parameters of this circuit are the same as those of a three-phase star rectifier (therefore not separately listed in Table 10.3). Furthermore, a star-connected primary winding with no neutral connection

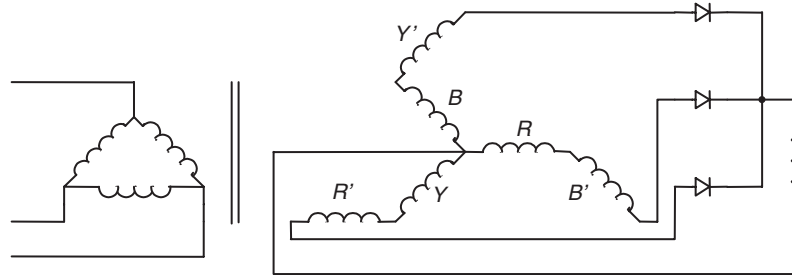


FIGURE 10.9 Three-phase inter-star rectifier.

is equally permissible because the sum of all primary phase currents is zero at all times.

10.3.1.3 Three-phase Double-star Rectifier with Inter-phase Transformer

This circuit consists essentially of two three-phase star rectifiers with their neutral points interconnected through an inter-phase transformer or reactor (Fig. 10.10). The polarities of the corresponding secondary windings in the two interconnected systems are reversed with respect to each other, so that the rectifier output voltage of one three-phase unit is at a minimum when the rectifier output voltage of the other unit is at a maximum as shown in Fig. 10.11. The function of the inter-phase transformer is to cause the output voltage v_L to be the average of the rectified voltages v_1 and v_2 as shown in Fig. 10.11. In addition, the ripple frequency of the output voltage is now six times that of the mains and therefore the component size of the filter (if there is any) becomes smaller. In a balanced circuit, the output currents of two three-phase units flowing in opposite directions in the inter-phase transformer winding will produce no dc magnetization current. Similarly, the dc magnetization currents in the secondary windings of two three-phase units cancel each other out.

By virtue of the symmetry of the secondary circuits, the three primary currents add up to zero at all times. Therefore, a star primary winding with no neutral connection would be equally permissible.

10.3.2 Three-phase Bridge Rectifiers

Three-phase bridge rectifiers are commonly used for high power applications because they have the highest possible transformer utilization factor for a three-phase system. The circuit of a three-phase bridge rectifier is shown in Fig. 10.12.

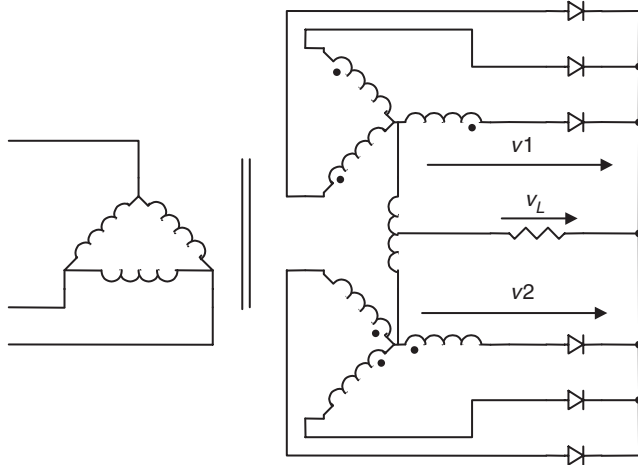


FIGURE 10.10 Three-phase double-star rectifier with inter-phase transformer.

The diodes are numbered in the order of conduction sequences and the conduction angle of each diode is $2\pi/3$.

The conduction sequence for diodes is 12, 23, 34, 45, 56, and 61. The voltage and the current waveforms of the three-phase bridge rectifier are shown in Fig. 10.13. The line voltage is 1.73 times the phase voltage of a three-phase star-connected source. It is permissible to use any combination of star- or delta-connected primary and secondary windings because the currents associated with the secondary windings are symmetrical.

Using Eq. (10.1) the average value of the output can be found as

$$V_{dc} = \frac{6}{2\pi} \int_{\pi/3}^{2\pi/3} \sqrt{3} V_m \sin \theta d\theta \quad (10.47)$$

or

$$V_{dc} = V_m \frac{3\sqrt{3}}{\pi} = 1.654 V_m \quad (10.48)$$

Similarly, using Eq. (10.6), the rms value of the output voltage can be found as

$$V_L = \sqrt{\frac{9}{\pi} \int_{\pi/3}^{2\pi/3} (V_m \sin \theta)^2 d\theta} \quad (10.49)$$

or

$$V_L = V_m \sqrt{\frac{3}{2} + \frac{9\sqrt{3}}{4\pi}} = 1.655 V_m \quad (10.50)$$

In addition, the rms current in each transformer secondary winding can also be found as

$$I_s = I_m \sqrt{\frac{2}{\pi} \left(\frac{\pi}{6} + \frac{\sqrt{3}}{4} \right)} = 0.78 I_m \quad (10.51)$$

and the rms current through a diode is

$$I_D = I_m \sqrt{\frac{1}{\pi} \left(\frac{\pi}{6} + \frac{\sqrt{3}}{4} \right)} = 0.552 I_m \quad (10.52)$$

where $I_m = 1.73 V_m / R$.

Based on Eqs. (10.48), (10.50), (10.51), and (10.52), all the important design parameters of the three-phase star rectifier can be evaluated, as listed in Table 10.3. The dc output voltage is slightly lower than the peak line voltage or 2.34 times the rms phase voltage. The V_{RRM} rating of the employed diodes is 1.05 times the dc output voltage, and the I_{FRM} rating of the employed diodes is 0.579 times the dc output current. Therefore, this three-phase bridge rectifier is very efficient and

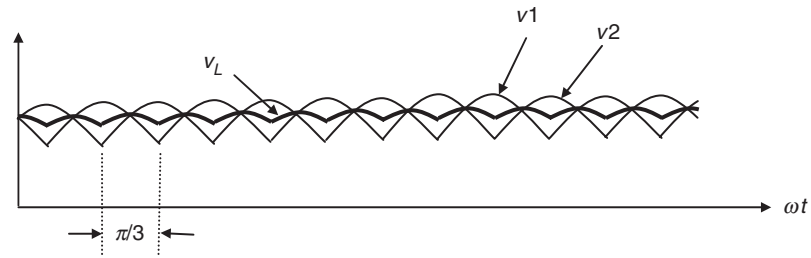


FIGURE 10.11 Voltage waveforms of the three-phase double-star rectifier.

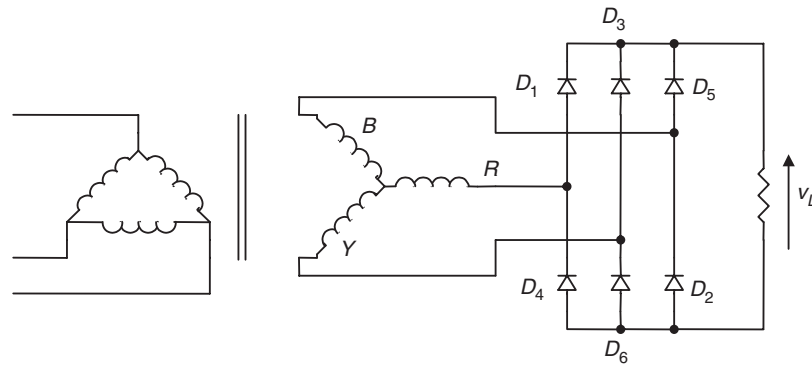


FIGURE 10.12 Three-phase bridge rectifier.

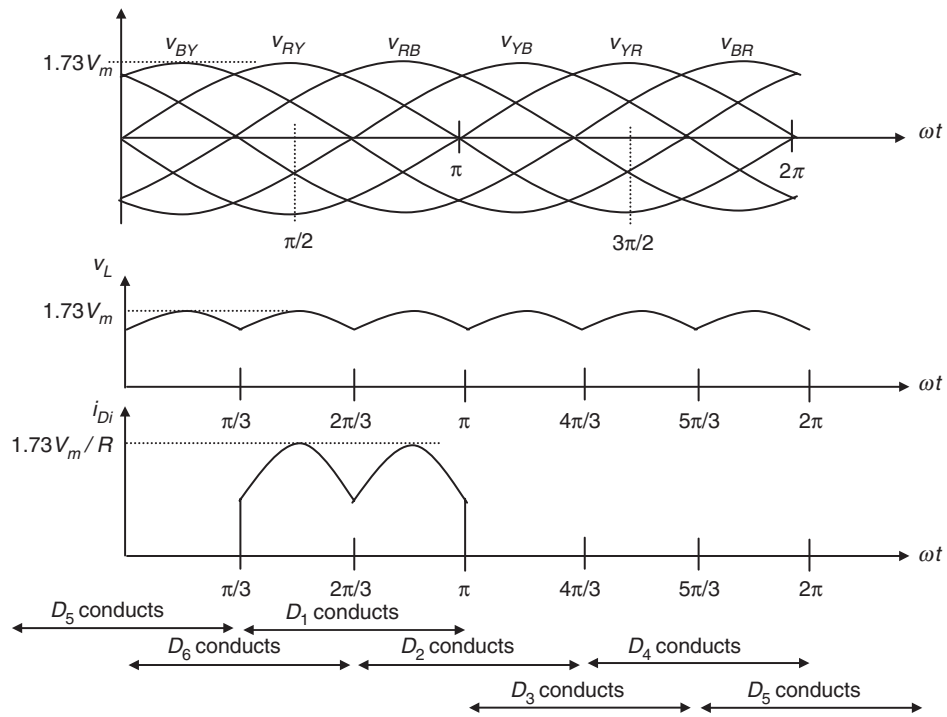


FIGURE 10.13 Voltage and current waveforms of the three-phase bridge rectifier.

popular wherever both dc voltage and current requirements are high. In many applications, no additional filter is required because the output ripple voltage is only 4.2%. Even if a filter is required, the size of the filter is relatively small because the ripple frequency is increased to six times the input frequency.

10.3.3 Operation of Rectifiers with Finite Source Inductance

It has been assumed in the preceding sections that the commutation of current from one diode to the next takes place instantaneously when the inter-phase voltage assumes the necessary polarity. In practice this is hardly possible, because there are finite inductances associated with the source. For the purpose of discussing the effects of the finite source inductance, a three-phase star rectifier with transformer leakage inductances is shown in Fig. 10.14, where l_1 , l_2 , l_3 denote the leakage inductances associated with the transformer secondary windings.

Refer to Fig. 10.15. At the time when v_{YN} is about to become larger than v_{RN} , due to leakage inductance l_1 , the current in D_1 cannot fall to zero immediately. Similarly, due to the leakage inductance l_2 , the current in D_2 cannot increase immediately

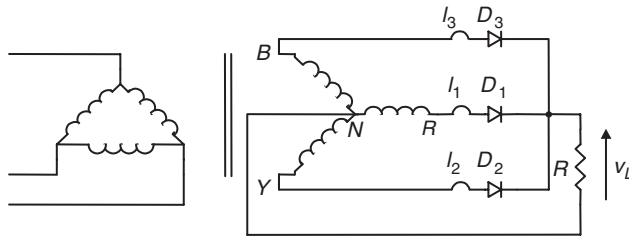


FIGURE 10.14 Three-phase star rectifier with the transformer leakage inductances.

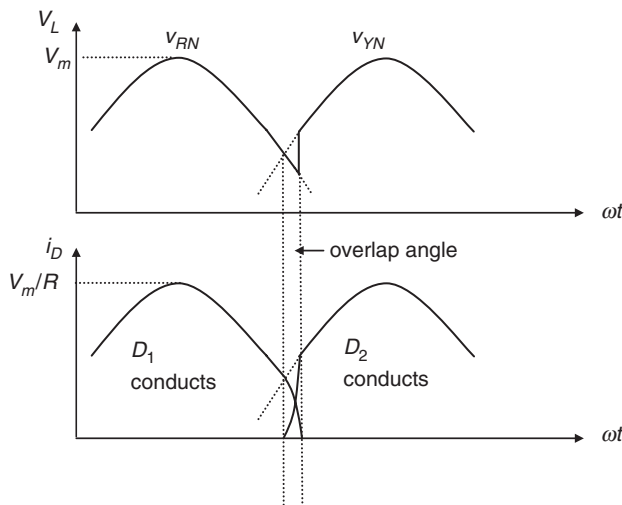


FIGURE 10.15 Waveforms during commutation in Fig. 10.14.

to the full value. The result is that both the diodes conduct for a certain period, which is called the overlap (or commutation) angle. The overlap reduces the rectified voltage v_L as shown in the upper voltage waveform of Fig. 10.15. If all the leakage inductances are equal, i.e. $l_1 = l_2 = l_3 = l_c$, then the amount of reduction of dc output voltage can be estimated as $mf_l I_{dc}$, where m is the ratio of the lowest-ripple frequency to the input frequency.

For example, for a three-phase star rectifier operating from a 60-Hz supply with an average load current of 50 A, the amount of reduction of the dc output voltage is 2.7 V if the leakage inductance in each secondary winding is 300 μ H.

10.4 Poly-phase Diode Rectifiers

10.4.1 Six-phase Star Rectifier

A basic six-phase star rectifier circuit is shown in Fig. 10.16. The six-phase voltages on the secondary are obtained by means of a center-tapped arrangement on a star-connected three-phase winding. Therefore, it is sometimes referred to as a three-phase full-wave rectifier. The diode in a particular phase conducts during the period when the voltage on that phase is higher than that on the other phases. The voltage waveforms of each phase and the load are shown in Fig. 10.17. It is clear that, unlike the three-phase star rectifier circuit, the conduction angle of each diode is $\pi/3$, instead of $2\pi/3$. Currents flow in only one rectifying element at a time, resulting in a low average current, but a high peak to an average current ratio in the diodes and poor transformer secondary utilization. Nevertheless, the dc currents in the secondary of the six-phase star rectifier cancel in the secondary windings like a full-wave rectifier and, therefore, core saturation is not encountered. This six-phase star circuit is attractive in applications which require a low ripple factor and a common cathode or anode for the rectifiers.

By considering the output voltage provided by v_{RN} between $\pi/3$ and $2\pi/3$, the average value of the output voltage can be

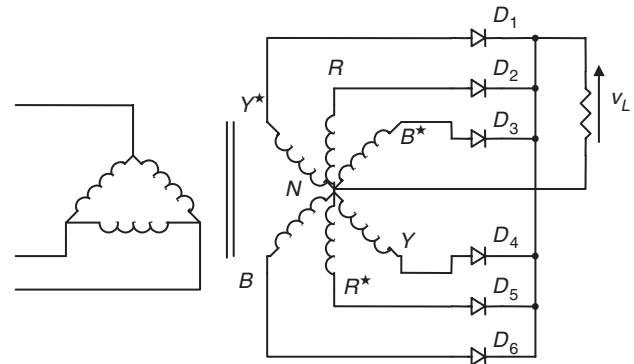


FIGURE 10.16 Six-phase star rectifier.

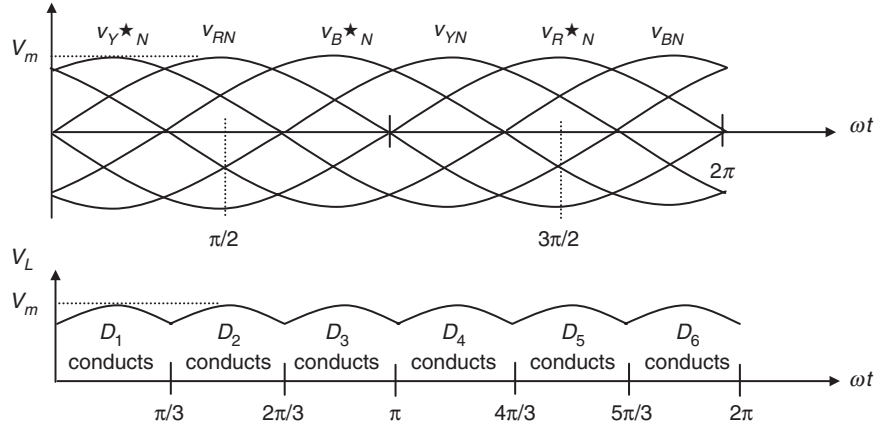


FIGURE 10.17 Voltage waveforms of the six-phase star rectifier.

found as

$$V_{dc} = \frac{6}{2\pi} \int_{\pi/3}^{2\pi/3} V_m \sin \theta d\theta \quad (10.53)$$

or

$$V_{dc} = V_m \frac{6}{\pi} \frac{1}{2} = 0.955 V_m \quad (10.54)$$

Similarly, the rms value of the output voltage can be found as

$$V_L = \sqrt{\frac{6}{2\pi} \int_{\pi/3}^{2\pi/3} (V_m \sin \theta)^2 d\theta} \quad (10.55)$$

or

$$V_L = V_m \sqrt{\frac{6}{2\pi} \left(\frac{\pi}{6} + \frac{\sqrt{3}}{4} \right)} = 0.956 V_m \quad (10.56)$$

In addition, the rms current in each transformer secondary winding can also be found as

$$I_s = I_m \sqrt{\frac{1}{2\pi} \left(\frac{\pi}{6} + \frac{\sqrt{3}}{4} \right)} = 0.39 I_m \quad (10.57)$$

where $I_m = V_m/R$.

Based on the relationships stated in Eqs. (10.55), (10.56), and (10.57), all the important design parameters of the six-phase star rectifier can be evaluated, as listed in Table 10.4 (given at the end of Subsection 10.4.3).

10.4.2 Six-phase Series Bridge Rectifier

The star- and delta-connected secondaries have an inherent $\pi/6$ -phase displacement between their output voltages. When a star- and a delta-connected bridge rectifier are connected

TABLE 10.4 Important design parameters of the six-phase rectifier circuits with resistive load

	Six-phase star rectifier	Six-phase series bridge rectifier	Six-phase parallel bridge rectifier (with inter-phase transformer)
Peak repetitive reverse voltage V_{RRM}	$2.09 V_{dc}$	$0.524 V_{dc}$	$1.05 V_{dc}$
RMS input voltage per transformer leg V_s	$0.74 V_{dc}$	$0.37 V_{dc}$	$0.715 V_{dc}$
Diode average current $I_{F(AV)}$	$0.167 I_{dc}$	$0.333 I_{dc}$	$0.167 I_{dc}$
Peak repetitive forward current I_{FRM}	$6.28 I_{F(AV)}$	$3.033 I_{F(AV)}$	$3.14 I_{F(AV)}$
Diode rms current $I_{F(RMS)}$	$0.409 I_{dc}$	$0.576 I_{dc}$	$0.409 I_{dc}$
Form factor of diode current $I_{F(RMS)}/I_{F(AV)}$	2.45	1.73	2.45
Rectification ratio	0.998	1.00	1.00
Form factor	1.0009	1.00005	1.00005
Ripple factor	0.042	0.01	0.01
Transformer rating primary VA	$1.28 P_{dc}$	$1.01 P_{dc}$	$1.01 P_{dc}$
Transformer rating secondary VA	$1.81 P_{dc}$	$1.05 P_{dc}$	$1.05 P_{dc}$
Output ripple frequency f_r	$6f_i$	$12f_i$	$12f_i$

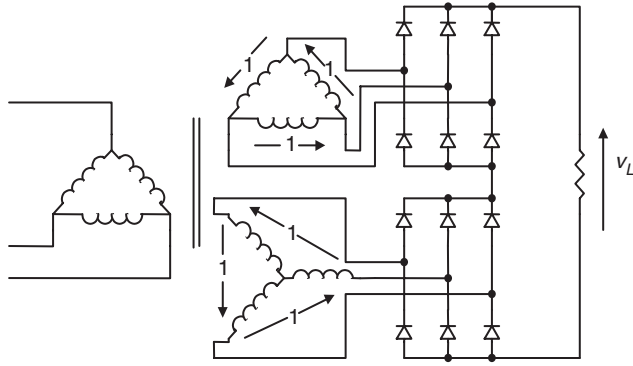


FIGURE 10.18 Six-phase series bridge rectifier.

in series as shown in Fig. 10.18, the combined output voltage will have a doubled ripple frequency (12 times that of the mains). The ripple of the combined output voltage will also be reduced from 4.2% (for each individual bridge rectifier) to 1%. The combined bridge rectifier is referred to as a six-phase series bridge rectifier.

In the six-phase series bridge rectifier shown in Fig. 10.18, let V_m^* be the peak voltage of the delta-connected secondary. The peak voltage between the lines of the star-connected secondary is also V_m^* . The peak voltage across the load, denoted as V_m , is equal to $2V_m^* \times \cos(\pi/12)$ or $1.932V_m^*$ because there is $\pi/6$ -phase displacement between the secondaries. The ripple frequency is twelve times the mains frequency. The average value of the output voltage can be found as

$$V_{dc} = \frac{12}{2\pi} \int_{5\pi/12}^{7\pi/12} V_m \sin \theta d\theta \quad (10.58)$$

or

$$V_{dc} = V_m \frac{12}{\pi} \frac{\sqrt{3}-1}{2\sqrt{2}} = 0.98862 V_m \quad (10.59)$$

The rms value of the output voltage can be found as

$$V_L = \sqrt{\frac{12}{2\pi} \int_{5\pi/12}^{7\pi/12} (V_m \sin \theta)^2 d\theta} \quad (10.60)$$

or

$$V_L = V_m \sqrt{\frac{12}{2\pi} \left(\frac{\pi}{12} + \frac{1}{4} \right)} = 0.98867 V_m \quad (10.61)$$

The rms current in each transformer secondary winding is

$$I_s = I_m \sqrt{\frac{4}{\pi} \left(\frac{\pi}{12} + \frac{1}{4} \right)} = 0.807 I_m \quad (10.62)$$

The rms current through a diode is

$$I_s = I_m \sqrt{\frac{2}{\pi} \left(\frac{\pi}{12} + \frac{1}{4} \right)} = 0.57 I_m \quad (10.63)$$

where $I_m = V_m/R$.

Based on Eqs. (10.59), (10.61), (10.62), and (10.63), all the important design parameters of the six-phase series bridge rectifier can be evaluated, as listed in Table 10.4 (given at the end of Subsection 10.4.3).

10.4.3 Six-phase Parallel Bridge Rectifier

The six-phase series bridge rectifier described above is useful for high output voltage applications. However, for high output current applications, the six-phase parallel bridge rectifier (with an inter-phase transformer) shown in Fig. 10.19 should be used.

The function of the inter-phase transformer is to cause the output voltage v_L to be the average of the rectified voltages v_1 and v_2 as shown in Fig. 10.20. As with the six-phase series

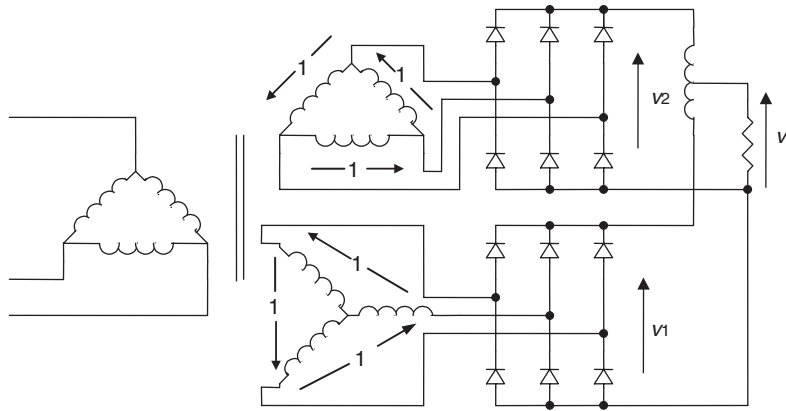


FIGURE 10.19 Six-phase parallel bridge rectifier.

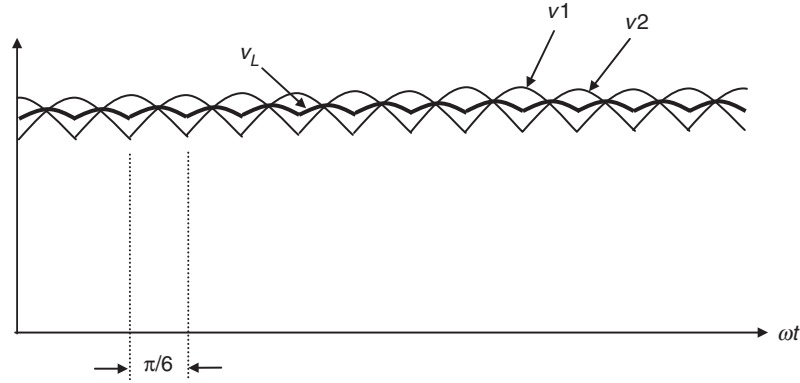


FIGURE 10.20 Voltage waveforms of the six-phase bridge rectifier with inter-phase transformer.

bridge rectifier, the output ripple frequency of the six-phase parallel bridge rectifier is also 12 times that of the mains. Further filtering on the output voltage is usually not required. Assuming a balanced circuit, the output currents of two three-phase units (flowing in opposite directions in the inter-phase transformer winding) produce no dc magnetization current.

All the important design parameters of the six-phase parallel rectifiers with inter-phase transformer are also listed in Table 10.4.

10.5 Filtering Systems in Rectifier Circuits

Filters are commonly employed in rectifier circuits for smoothing out the dc output voltage of the load. They are classified as inductor-input dc filters and capacitor-input dc filters. Inductor-input dc filters are preferred in high-power applications because more efficient transformer operation is obtained due to the reduction in the form factor of the rectifier current. Capacitor-input dc filters can provide volumetrically efficient operation, but they demand excessive turn-on and repetitive surge currents. Therefore, capacitor-input dc filters are suitable only for lower-power systems where close regulation is usually achieved by an electronic regulator cascaded with the rectifier.

10.5.1 Inductive-input DC Filters

The simplest inductive-input dc filter is shown in Fig. 10.21a. The output current of the rectifier can be maintained at a steady value if the inductance of L_f is sufficiently large ($\omega L_f \gg R$). The filtering action is more effective in heavy load conditions than in light load conditions. If the ripple attenuation is not sufficient even with large values of inductance, an L-section filter as shown in Fig. 10.21b can be used for further filtering. In practice, multiple L-section filters can also be employed if the requirement on the output ripple is very stringent.

For a simple inductive-input dc filter shown in Fig. 10.21a, the ripple is reduced by the factor

$$\frac{v_o}{v_L} = \frac{R}{\sqrt{R^2 + (2\pi f_r L_f)^2}} \quad (10.64)$$

where v_L is the ripple voltage before filtering, v_o is the ripple voltage after filtering, and f_r is the ripple frequency.

For the inductive-input dc filter shown in Fig. 10.21b, the amount of reduction in the ripple voltage can be estimated as

$$\frac{v_o}{v_L} = \left| \frac{1}{1 - (2\pi f_r)^2 L_f C_f} \right| \quad (10.65)$$

where f_r is the ripple frequency, if $R \gg 1/2\pi f_r C_f$.

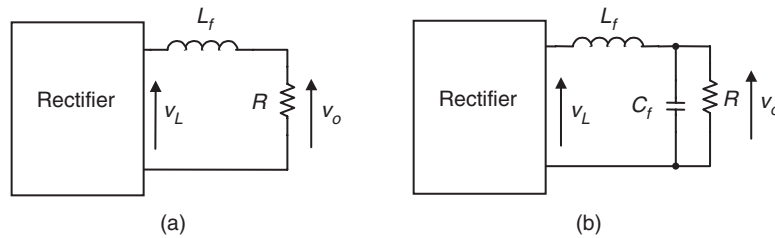


FIGURE 10.21 Inductive-input dc filters.

10.5.1.1 Voltage and Current Waveforms of Full-wave Rectifier with Inductor-input DC Filter

Figure 10.22 shows a single-phase full-wave rectifier with an inductor-input dc filter. The voltage and current waveforms are illustrated in Fig. 10.23.

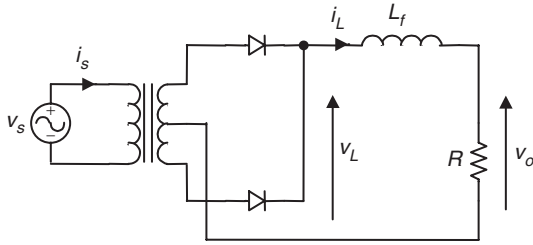


FIGURE 10.22 A full-wave rectifier with inductor-input dc filter.

When the inductance of L_f is infinite, the current through the inductor and the output voltage are constant. When inductor L_f is finite, the current through the inductor has a ripple component, as shown by the dotted lines in Fig. 10.23. If the input inductance is too small, the current decreases to zero (becoming discontinuous) during a portion of the time between the peaks of the rectifier output voltage. The minimum value of inductance required to maintain a continuous current is known as the critical inductance L_C .

10.5.1.2 Critical inductance L_C

In the case of single-phase full-wave rectifiers, the critical inductance can be found as

$$\text{Full-wave } L_C = \frac{R}{6\pi f_i} \quad (10.66)$$

where f_i is the input mains frequency.

In the case of poly-phase rectifiers, the critical inductance can be found as

$$\text{Poly-phase } L_C = \frac{R}{3\pi m(m^2 - 1)f_i} \quad (10.67)$$

where m is ratio of the lowest ripple frequency to the input frequency, e.g. $m = 6$ for a three-phase bridge rectifier.

10.5.1.3 Determining the Input Inductance for a Given Ripple Factor

In practice, the choice of the input inductance depends on the required ripple factor of the output voltage. The ripple voltage of a rectifier without filtering can be found by means of Fourier Analysis. For example, the coefficient of the n th harmonic component of the rectified voltage v_L shown in Fig. 10.22 can be expressed as:

$$v_{L_n} = \frac{-4V_m}{\pi(n^2 - 1)} \quad (10.68)$$

where $n = 2, 4, 8, \dots$ etc.

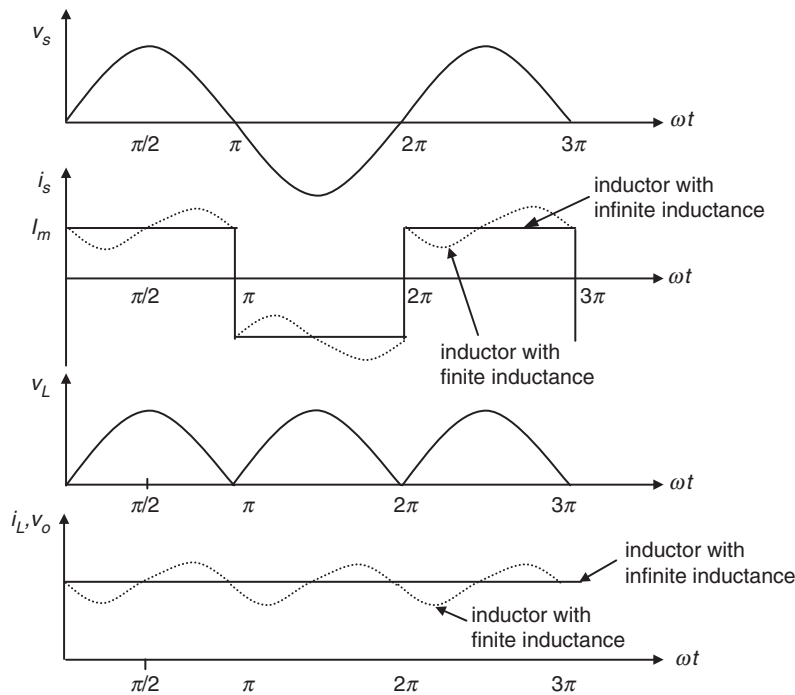


FIGURE 10.23 Voltage and current waveforms of full-wave rectifier with inductor-input dc filter.

The dc component of the rectifier voltage is given by Eq. (10.5). Therefore, in addition to Eq. (10.27), the ripple factor can also be expressed as

$$RF = \sqrt{2 \sum_{n=2,4,8} \left(\frac{1}{n^2 - 1} \right)^2} \quad (10.69)$$

Considering only the lowest-order harmonic ($n = 2$), the output ripple factor of a simple inductor-input dc filter (without C_f) can be found, from Eqs. (10.64) and (10.69), as

$$\text{Filtered RF} = \frac{0.4714}{\sqrt{1 + (4\pi f_i L_f / R)^2}} \quad (10.70)$$

10.5.1.4 Harmonics of the Input Current

In general, the total harmonic distortion (THD) of an input current is defined as

$$\text{THD} = \sqrt{\left(\frac{I_s}{I_{s1}} \right)^2 - 1} \quad (10.71)$$

where I_s is the rms value of the input current and I_{s1} and the rms value of the fundamental component of the input current. The THD can also be expressed as

$$\text{THD} = \sqrt{\sum_{n=2,3,4} \left(\frac{I_{sn}}{I_{s1}} \right)^2} \quad (10.72)$$

where I_{sn} is the rms value of the n th harmonic component of the input current.

Moreover, the input power factor is defined as

$$\text{PF} = \frac{I_{s1}}{I_s} \cos \phi \quad (10.73)$$

where ϕ is the displacement angle between the fundamental components of the input current and voltage.

Assume that inductor L_f of the circuit shown in Fig. 10.22 has an infinitely large inductance. The input current is then a square wave. This input current contains undesirable higher harmonics that reduce the input power factor of the system. The input current can be easily expressed as

$$i_s = \frac{4I_m}{\pi} \sum_{n=1,3,5} \frac{1}{n} \sin 2n\pi f_i t \quad (10.74)$$

The rms values of the input current and its fundamental component are I_m and $4I_m/(\pi\sqrt{2})$ respectively. Therefore, the THD of the input current of this circuit is 0.484. Since the displacement angle $\phi = 0$, the power factor is $4/(\pi\sqrt{2}) = 0.9$.

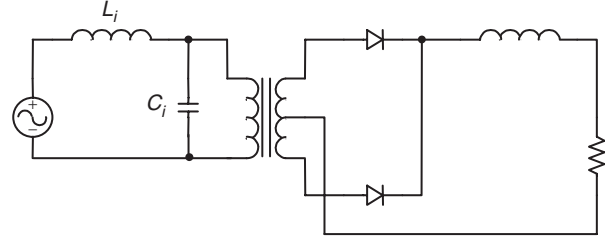


FIGURE 10.24 Rectifier with input ac filter.

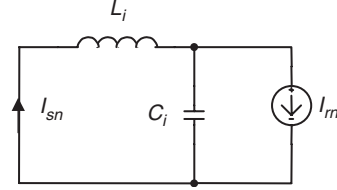


FIGURE 10.25 Equivalent circuit for input ac filter.

The power factor of the circuit shown in Fig. 10.22 can be improved by installing an ac filter between the source and the rectifier, as shown in Fig. 10.24.

Considering only the harmonic components, the equivalent circuit of the rectifier given in Fig. 10.24 can be found as shown in Fig. 10.25. The rms value of the n th harmonic current appearing in the supply can then be obtained using the current-divider rule,

$$I_{sn} = \left| \frac{1}{1 - (2n\pi f_i)^2 L_i C_i} \right| I_m \quad (10.75)$$

where I_{rn} is the rms value of the n th harmonic current of the rectifier.

Applying Eq. (10.73) and knowing $I_{rn}/I_{r1} = 1/n$ from Eq. (10.74), the THD of the rectifier with input filter shown in Fig. 10.24 can be found as

$$\text{Filtered THD} = \sqrt{\sum_{n=3,5} \frac{1}{n^2} \left| \frac{1}{1 - (2n\pi f_i)^2 L_i C_i} \right|^2} \quad (10.76)$$

The important design parameters of typical single-phase and three-phase rectifiers with inductor-input dc filter are listed in Table 10.5. Note that, in a single-phase half-wave rectifier, a freewheeling diode is required to be connected across the input of the dc filters such that the flow of load current can be maintained during the negative half-cycle of the supply voltage.

10.5.2 Capacitive-input DC Filters

Figure 10.26 shows a full-wave rectifier with capacitor-input dc filter. The voltage and current waveforms of this rectifier

TABLE 10.5 Important design parameters of typical rectifier circuits with inductor-input dc filter

	Full-wave rectifier with center-tapped transformer	Full-wave bridge rectifier	Three-phase star rectifier	Three-phase bridge rectifier	Three-phase double-star rectifier with inter-phase transformer
Peak repetitive reverse voltage V_{RRM}	$3.14V_{dc}$	$1.57V_{dc}$	$2.09V_{dc}$	$1.05V_{dc}$	$2.42V_{dc}$
RMS input voltage per transformer leg V_s	$1.11V_{dc}$	$1.11V_{dc}$	$0.885V_{dc}$	$0.428V_{dc}$	$0.885V_{dc}$
Diode average current $I_{F(AV)}$	$0.5I_{dc}$	$0.5I_{dc}$	$0.333I_{dc}$	$0.333I_{dc}$	$0.167I_{dc}$
Peak repetitive forward current I_{FRM}	$2.00I_{F(AV)}$	$2.00I_{F(AV)}$	$3.00I_{F(AV)}$	$3.00I_{F(AV)}$	$3.00I_{F(AV)}$
Diode rms current $I_{F(RMS)}$	$0.707I_{dc}$	$0.707I_{dc}$	$0.577I_{dc}$	$0.577I_{dc}$	$0.289I_{dc}$
Form factor of diode current $I_{F(RMS)}/I_{F(AV)}$	1.414	1.414	1.73	1.73	1.73
Transformer rating primary VA	$1.11P_{dc}$	$1.11P_{dc}$	$1.21P_{dc}$	$1.05P_{dc}$	$1.05P_{dc}$
Transformer rating secondary VA	$1.57P_{dc}$	$1.11P_{dc}$	$1.48P_{dc}$	$1.05P_{dc}$	$1.48P_{dc}$
Output ripple frequency f_r	$2f_i$	$2f_i$	$3f_i$	$6f_i$	$6f_i$
Ripple component V_r at					
(a) fundamental,	$0.667V_{dc}$	$0.667V_{dc}$	$0.250V_{dc}$	$0.057V_{dc}$	$0.057V_{dc}$
(b) second harmonic,	$0.133V_{dc}$	$0.133V_{dc}$	$0.057V_{dc}$	$0.014V_{dc}$	$0.014V_{dc}$
(c) third harmonic of the ripple frequency	$0.057V_{dc}$	$0.057V_{dc}$	$0.025V_{dc}$	$0.006V_{dc}$	$0.006V_{dc}$

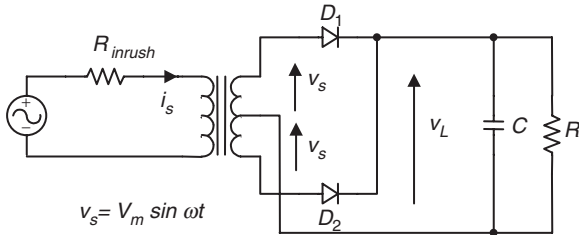


FIGURE 10.26 Full-wave rectifier with capacitor-input dc filter.

are shown in Fig. 10.27. When the instantaneous voltage of the secondary winding v_s is higher than the instantaneous value of capacitor voltage v_L , either D_1 or D_2 conducts, and the capacitor C is charged up from the transformer. When the instantaneous voltage of the secondary winding v_s falls below the instantaneous value of capacitor voltage v_L , both the diodes are reverse biased and the capacitor C is discharged through load resistance R . The resulting capacitor voltage v_L varies between a maximum value of V_m and a minimum value of $V_m - V_{r(pp)}$ as shown in Fig. 10.27. ($V_{r(pp)}$ is the peak-to-peak ripple voltage.) As shown in Fig. 10.27, the conduction angle θ_c of the diodes becomes smaller when the output-ripple voltage decreases. Consequently, the power supply and the diodes suffer from high repetitive surge currents. An LC ac filter, as shown in Fig. 10.24, may be required to improve the input power factor of the rectifier.

In practice, if the peak-to-peak ripple voltage is small, it can be approximated as

$$V_{r(pp)} = \frac{V_m}{f_r RC} \quad (10.77)$$

where f_r is the output ripple frequency of the rectifier.

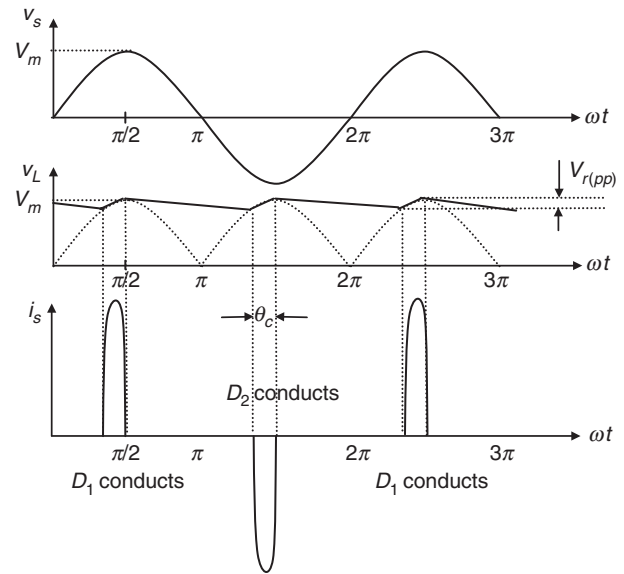


FIGURE 10.27 Voltage and current waveforms of the full-wave rectifier with capacitor-input dc filter.

Therefore, the average output voltage V_{dc} is given by

$$V_{dc} = V_m \left(1 - \frac{1}{2f_r RC} \right) \quad (10.78)$$

The rms output ripple voltage V_{ac} is approximately given by

$$V_{ac} = \frac{V_m}{2\sqrt{2}f_r RC} \quad (10.79)$$

The ripple factor RF can be found from

$$RF = \frac{1}{\sqrt{2}(2f_r RC - 1)} \quad (10.80)$$

10.5.2.1 Inrush Current

The resistor R_{inrush} in Fig. 10.26 is used to limit the inrush current imposed on the diodes during the instant when the rectifier is being connected to the supply. The inrush current can be very large because capacitor C has zero charge initially. The worst case occurs when the rectifier is connected to the supply at its maximum voltage. The worst-case inrush current can be estimated from

$$I_{inrush} = \frac{V_m}{R_{sec} + R_{ESR}} \quad (10.81)$$

where R_{sec} is the equivalent resistance looking from the secondary transformer and R_{ESR} is the equivalent series resistance (ESR) of the filtering capacitor. Hence the employed diode should be able to withstand the inrush current for a half cycle of the input voltage. In other words, the *Maximum Allowable Surge Current* (I_{FSM}) rating of the employed diodes must be higher than the inrush current. The equivalent resistance associated with the transformer windings and the filtering capacitor is usually sufficient to limit the inrush current to an acceptable level. However, in cases where the transformer is omitted, e.g. the rectifier of an off-line switch-mode supply, resistor R_{inrush} must be added for controlling the inrush current.

Consider as an example, a single-phase bridge rectifier, which is to be connected to a 120-V–60-Hz source (without transformer). Assume that the I_{FSM} rating of the diodes is 150 A for an interval of 8.3 ms. If the ESR of the filtering capacitor is zero, the value of the resistor for limiting inrush current resistance can be estimated to be 1.13 Ω using Eq. (10.81).

10.6 High-frequency Diode Rectifier Circuits

In high-frequency converters, diodes perform various functions, such as rectifying, flywheeling, and clamping. One special quality a high-frequency diode must possess is a fast switching speed. In technical terms, it must have a short reverse recovery time and a short forward recovery time.

The reverse recovery time of a diode may be understood as the time a forwardly conducting diode takes to recover to a blocking state when the voltage across it is suddenly reversed

(which is known as forced turn-off). The temporary short circuit during the reverse recovery period may result in large reverse current, excessive ringing, and large power dissipation, all of which are highly undesirable.

The forward recovery time of a diode may be understood as the time a non-conducting diode takes to change to the fully-on state when a forward current is suddenly forced into it (which is known as forced turn-on). Before the diode reaches the fully-on state, the forward voltage drop during the forward recovery time can be significantly higher than the normal on-state voltage drop. This may cause voltage spikes in the circuit.

It should be interesting to note that, as far as circuit operation is concerned, a diode with a long reverse recovery time is similar to a diode with a large parasitic capacitance. A diode with a long forward recovery time is similar to a diode with a large parasitic inductance. (Spikes caused by the slow forward recovery of diodes are often wrongly thought to be caused by leakage inductance.) Comparatively, the adverse effect of a long reverse recovery time is much worse than that of a long forward recovery time.

Among commonly used diodes, the Schottky diode has the shortest forward and reverse recovery times. Schottky diodes are therefore most suitable for high-frequency applications. However, Schottky diodes have relatively low reverse breakdown voltage (normally lower than 200 V) and large leakage current. If, due to these limitations, Schottky diodes cannot be used, ultra-fast diodes should be used in high-frequency converter circuits.

Using the example of a forward converter, the operations of a forward rectifier diode, a flywheel diode, and a clamping diode will be studied in Subsection 10.6.1. Because of the difficulties encountered in the full analyses taking into account parasitic/stray/leakage components, PSpice simulations are extensively used here to study the following:

- The idealized operation of the converter.
- The adverse effects of relatively slow rectifiers (e.g. the so-called ultra-fast diodes, which are actually much slower than Schottky diodes).
- The improvement achievable by using high-speed rectifiers (Schottky diodes).
- The effects of leakage inductance of the transformer.
- The use of snubber circuits to reduce ringing.
- The operation of a practical converter with snubber circuits.

Using the example of a flyback converter, the operations of a flyback rectifier diode and a clamping diode will also be studied in Subsection 10.6.2.

The design considerations for high-frequency diode rectifier circuits will be discussed in Subsection 10.6.3. Some precautions which must be taken in the interpretation of computer simulation results are briefed in Subsection 10.6.4.

10.6.1 Forward Rectifier Diode, Flywheel Diode, and Magnetic-reset Clamping Diode in a Forward Converter

10.6.1.1 Ideal Circuit

Figure 10.28 shows the basic circuit of a forward converter. Figure 10.29 shows the idealized steady-state waveforms for continuous-mode operation (the current in L_1 being continuous). These waveforms are obtained from PSpice simulations, based on the following assumptions:

- Rectifier diode D_R , flywheel diode D_F , and magnetic-reset clamping diode D_M are ideal diodes with infinitely fast switching speed.
- Electronic switch M_1 is an idealized MOS switch with infinitely fast switching speed and

On-state resistance = 0.067Ω

Off-state resistance = $1 \text{ M}\Omega$

It should be noted that PSpice does not allow a switch to have zero on-state resistance and infinite off-state resistance.

- Transformer T_1 has a coupling coefficient of 0.99999999. PSpice does not accept a coupling coefficient of 1.
- The switching operation of the converter has reached a steady state.

Referring to the circuit shown in Fig. 10.28 and the waveforms shown in Fig. 10.29, the operation of the converter can be explained as follows:

1. For $0 < t < DT$ (D is the duty cycle of the MOS switch M_1 and T is the switching period of the converter. M_1 is turned on when $V_1(\text{VPULSE})$ is 15 V, and turned off when $V_1(\text{VPULSE})$ is 0 V).

The switch M_1 is turned on at $t = 0$.

The voltage at node 3, denoted as $V(3)$, is

$$V(3) = 0 \quad \text{for} \quad 0 < t < DT \quad (10.82)$$

The voltage induced at node 6 of the secondary winding L_S is

$$V(6) = V_{IN} (N_S/N_P) \quad (10.83)$$

This voltage drives a current $I(DR)$ (current through rectifier diode D_R) into the output circuit to produce the output voltage V_o . The rate of increase of $I(DR)$ is given by

$$\frac{dI(DR)}{dt} = \left[V_{IN} \frac{N_S}{N_P} - V_o \right] \frac{1}{L_1} \quad (10.84)$$

where V_o is the dc output voltage of the converter.

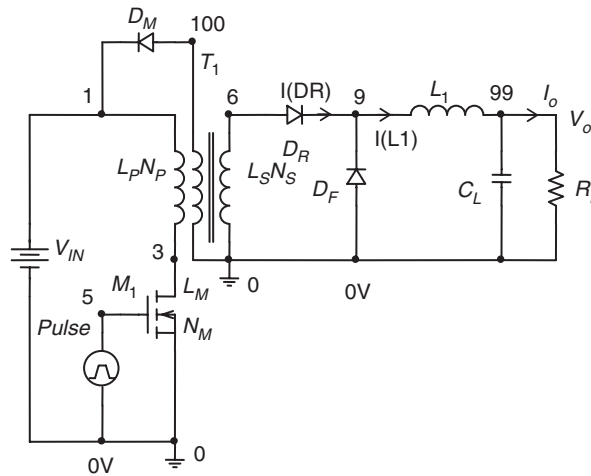
The flywheel diode D_F is reversely biased by $V(9)$, the voltage at node 9.

$$V(9) = V_{IN} (N_S/N_P) \quad \text{for} \quad 0 < t < DT \quad (10.85)$$

The magnetic-reset clamping diode D_M is reversely biased by the negative voltage at node 100. Assuming that L_M and L_P have the same number of turns, we have

$$V(100) = -V_{IN} \quad \text{for} \quad 0 < t < DT \quad (10.86)$$

A magnetizing current builds up linearly in L_P . This magnetizing current reaches the maximum value of $(V_{IN}DT)/L_P$ at $t = DT$.



Notes:

$$V_{IN} = 50 \text{ V}$$

$$L_1 = 8 \mu\text{H}$$

$$C_L = 300 \mu\text{F}$$

$$L_P = 0.576 \text{ mH}$$

$$L_M = 0.576 \text{ mH}$$

$$L_S = 0.036 \text{ mH}$$

$$R_L = 0.35 \Omega$$

$$N_P : N_M : N_S = 4 : 4 : 1$$

FIGURE 10.28 Basic circuit of forward converter.

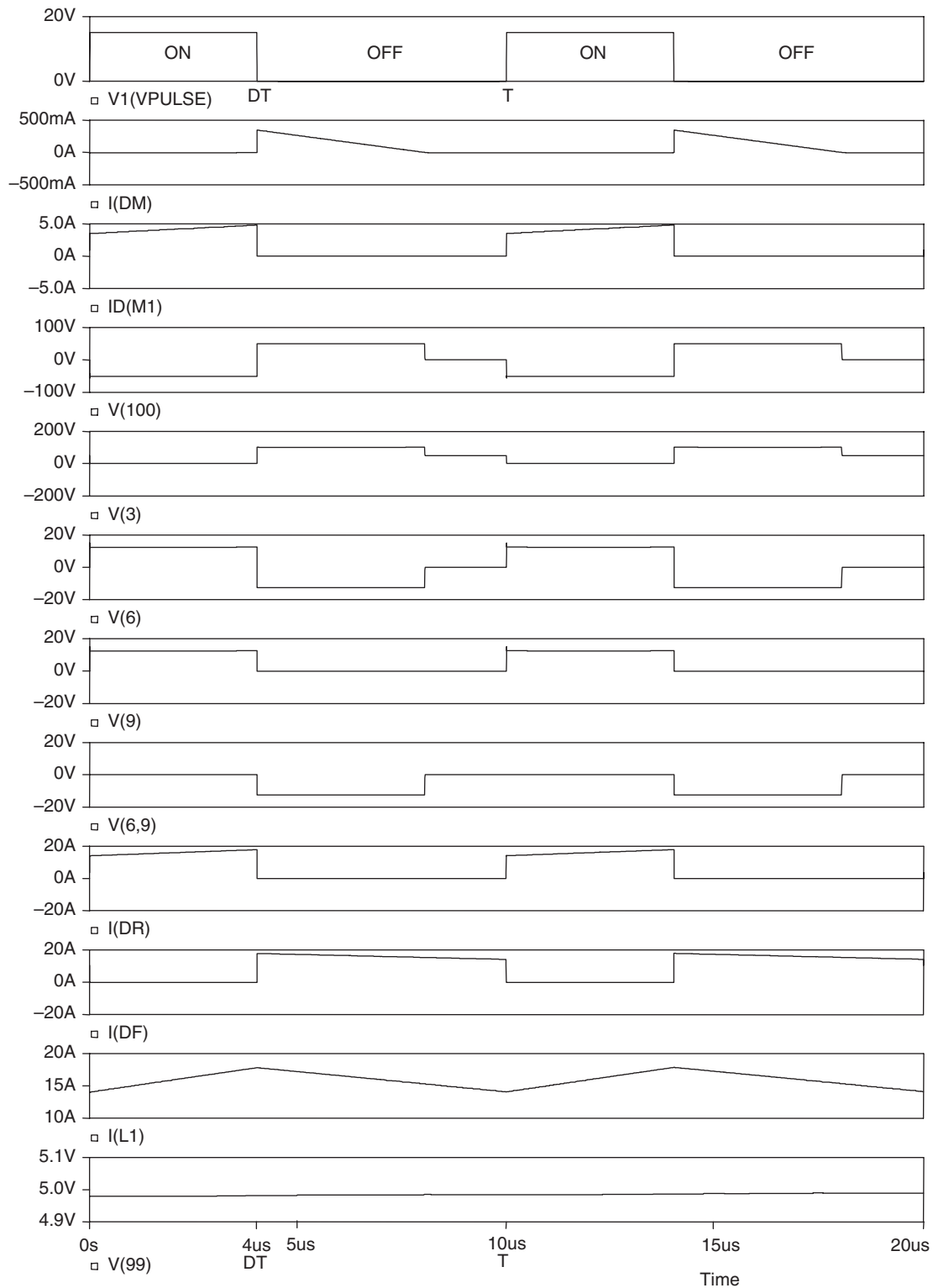


FIGURE 10.29 Idealized steady-state waveforms of forward converter for continuous-mode operation.

2. For $DT < t < 2DT$

The switch M_1 is turned off at $t = DT$.

The collapse of magnetic flux induces a back emf in L_M , which is equal to L_P , to turn-on the clamping diode D_M . The magnetizing current in L_M drops (from the maximum value of $(V_{IN}DT)/L_P$, as mentioned above) at the rate of V_{IN}/L_P . It reaches zero at $t = 2DT$.

The back emf induced across L_P is equal to V_{IN} . The voltage at node 3 is

$$V(3) = 2V_{IN} \quad \text{for } DT < t < 2DT \quad (10.87)$$

The back emf across L_S forces D_R to stop conducting.

The inductive current in L_1 forces the flywheel diode D_F to conduct. $I(L_1)$ (current through L_1) falls at the rate of

$$\frac{dI(L_1)}{dt} = \frac{-V_o}{L_1} \quad (10.88)$$

The voltage across D_R , denoted as $V(6,9)$ (the voltage at node 6 with respect to node 9), is

$$\begin{aligned} V(DR) &= V(6,9) \\ &= -V_{IN}(N_S/N_P) \quad \text{for } DT < t < 2DT \end{aligned} \quad (10.89)$$

3. For $2DT < t < T$

D_M stops conducting at $t = 2DT$. The voltage across L_M then falls to zero.

The voltage across L_P is zero.

$$V(3) = V_{IN} \quad (10.90)$$

The voltage across L_S is also zero.

$$V(6) = 0 \quad (10.91)$$

Inductive current $I(L_1)$ continues to fall at the rate of

$$\frac{dI(L_1)}{dt} = \frac{-V_o}{L_1} \quad (10.92)$$

The switching cycle restarts when the switch M_1 is turned on again at $t = T$.

From the waveforms shown in Fig. 10.29, the following useful information (for continuous-mode operation) can be found:

- The output voltage V_o is equal to the average value of $V(9)$.

$$V_o = D \frac{N_S}{N_P} V_{IN} \quad (10.93)$$

- The maximum current in the forward rectifying diode D_R and flywheel diode D_F is

$$\begin{aligned} I(DR)_{max} &= I(DF)_{max} \\ &= I_o + \frac{1}{2} \frac{V_o}{L_1} (1 - D) T \end{aligned} \quad (10.94)$$

where $V_o = DV_{IN}(N_S/N_P)$ and I_o is the output loading current.

- The maximum reverse voltage of D_R and D_F is

$$\begin{aligned} V(DR)_{max} &= V(DF)_{max} \\ &= V(6,9)_{max} = V_{IN} \frac{N_S}{N_P} \end{aligned} \quad (10.95)$$

- The maximum reverse voltage of D_M is

$$V(DM)_{max} = V_{IN} \quad (10.96)$$

- The maximum current in D_M is

$$I(DM)_{max} = DT \frac{V_{IN}}{L_P} \quad (10.97)$$

- The maximum current in the switch M_1 , denoted as $ID(M_1)$, is

$$\begin{aligned} ID(M_1)_{max} &= \frac{N_S}{N_P} I(DR)_{max} + I(DM)_{max} \\ &= \frac{N_S}{N_P} \left[I_o + \frac{1}{2} \frac{V_o}{L_1} (1 - D) T \right] + DT \frac{V_{IN}}{L_P} \end{aligned} \quad (10.98)$$

It should, however, be understood that, due to the non-ideal characteristics of practical components, the idealized waveforms shown in Fig. 10.29 cannot actually be achieved in the real world. In the following, the effects of non-ideal diodes and transformers will be examined.

10.6.1.2 Circuit Using Ultra-fast Diodes

Figure 10.30 shows the waveforms of the forward converter (circuit given in Fig. 10.28) when ultra-fast diodes are used as D_M , D_R , and D_F . (Note that ultra-fast diodes are actually much slower than Schottky diodes.) The waveforms are obtained by PSpice simulations, based on the following assumptions:

- D_M is an MUR460 ultra-fast diode. D_R and D_F are MUR1560 ultra-fast diodes.
- M_1 is an IRF640 MOS transistor.
- Transformer T_1 has a coupling coefficient of 0.99999999 (which may be assumed to be 1).
- The switching operation of the converter has reached a steady state.

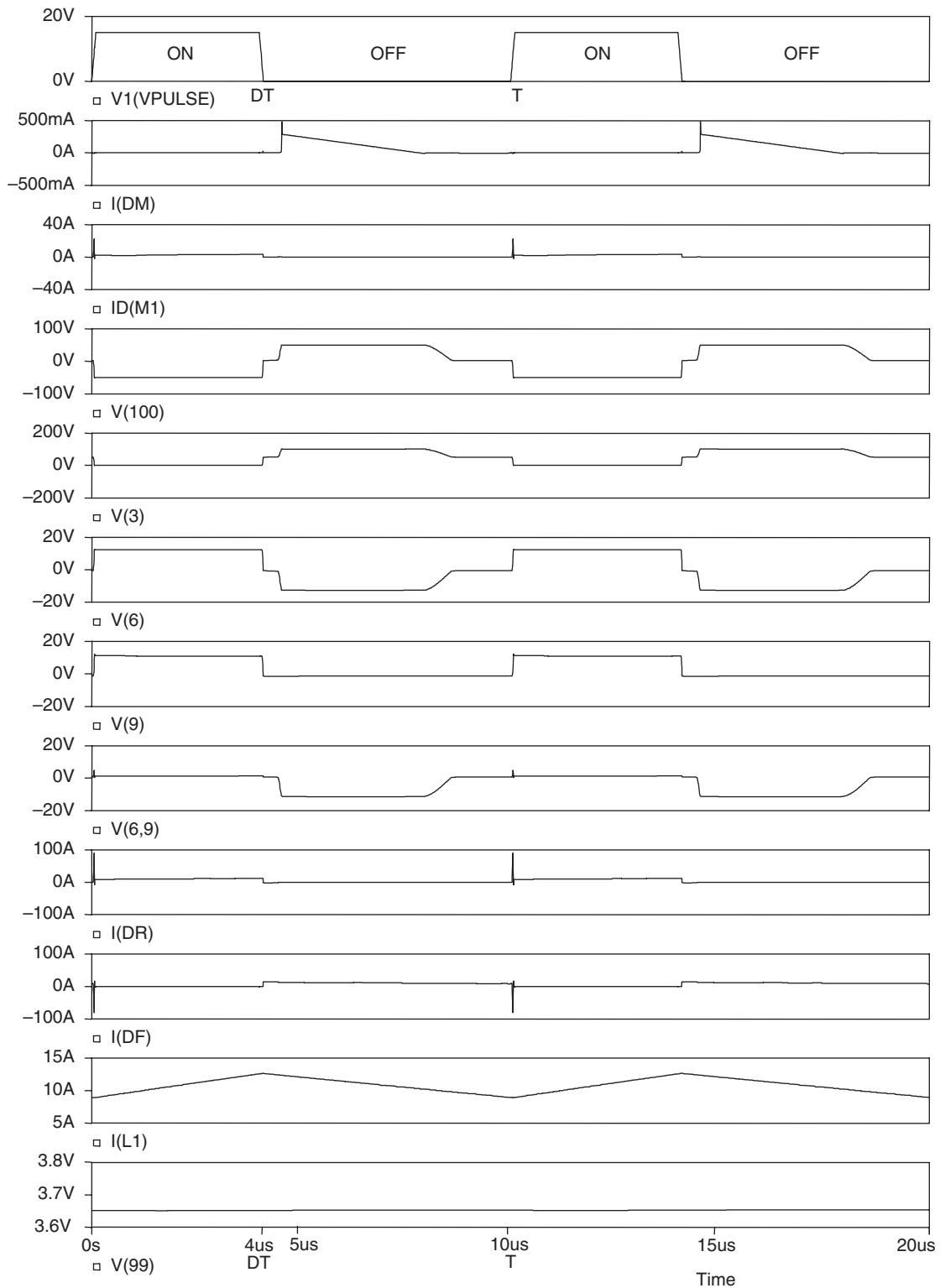


FIGURE 10.30 Waveforms of forward converter using “ultra-fast” diodes (which are actually much slower than Schottky diodes).

It is observed that a large spike appears in the current waveforms of diodes D_R and D_F (denoted as $I(DR)$ and $I(DF)$ in Fig. 10.30) whenever the MOS transistor M_1 is turned on. This is due to the relatively slow reverse recovery of the flywheel diode D_F . During the reverse recovery time, the positive voltage suddenly appearing across L_S (which is equal to $V_{IN}(N_S/N_P)$) drives a large transient current through D_R and D_F . This current spike results in large current stress and power dissipation in D_R , D_F , and M_1 .

A method of reducing the current spikes is to use Schottky diodes as D_R and D_F , as described below.

10.6.1.3 Circuit Using Schottky Diodes

In order to reduce the current spikes caused by the slow reverse recovery of rectifiers, Schottky diodes are now used as D_R and D_F . The assumptions made here are (referring to the circuit shown in Fig. 10.28):

- D_R and D_F are MBR2540 Schottky diodes.
- D_M is an MUR460 ultra-fast diode.
- M_1 is an IRF640 MOS transistor.
- Transformer T_1 has a coupling coefficient of 0.99999999.
- The switching operation of the converter has reached a steady state.

The new simulated waveforms are given in Fig. 10.31. It is found that, by employing Schottky diodes as D_R and D_F , the amplitudes of the current spikes in $I(DM)$, $I(DR)$, and $I(DF)$ can be reduced to practically zero. This solves the slow-speed problem of ultra-fast diodes.

10.6.1.4 Circuit with Practical Transformer

The simulation results given above in Figs. 10.29–10.31 (for the forward converter circuit shown in Fig. 10.28) are based on the assumption that transformer T_1 has effectively no leakage inductance (with coupling coefficient $K = 0.99999999$). It is, however, found that when a practical transformer (having a slightly lower K) is used, severe ringings occur. Figure 10.32 shows some simulation results to demonstrate this phenomenon, where the following assumptions are made:

- D_R and D_F are MBR2540 Schottky diodes. D_M is an MUR460 ultra-fast diode.
- M_1 is an IRF640 MOS transistor.
- Transformer T_1 has a practical coupling coefficient of 0.996.
- The effective winding resistance of L_P is $0.1\ \Omega$. The effective winding resistance of L_M is $0.4\ \Omega$. The effective winding resistance of L_S is $0.01\ \Omega$.
- The effective series resistance of the output filtering capacitor is $0.05\ \Omega$.
- The switching operation of the converter has reached a steady state.

The resultant waveforms shown in Fig. 10.32 indicate that there are large voltage and current ringings in the circuit. These ringings are caused by the resonant circuits formed by the leakage inductance of the transformer and the parasitic capacitances of diodes and transistor.

A practical converter may therefore need snubber circuits to damp these ringings, as described below.

10.6.1.5 Circuit with Snubber Across the Transformer

In order to suppress the ringing voltage caused by the resonant circuit formed by transformer leakage inductance and the parasitic capacitance of the MOS switch, a snubber circuit, shown as R_1 and C_1 in Fig. 10.33, is now connected across the primary winding of transformer T_1 . The new waveforms are shown in Fig. 10.34. Here the drain-to-source voltage waveform of the MOS transistor, $V(3)$, is found to be acceptable. However, there are still large ringing voltages across the output rectifiers ($V(6,9)$ and $V(9)$).

In order to damp the ringing voltages across the output rectifiers, additional snubber circuits across the rectifiers may therefore also be required in a practical circuit, as described below.

10.6.1.6 Practical Circuit

Figure 10.35 shows a practical forward converter with snubber circuits added also to rectifiers (R_2C_2 for D_R and R_3C_3 for D_F) to reduce the voltage ringing. Figures 10.36 and 10.37 show the resultant voltage and current waveforms. Figure 10.36 is for continuous-mode operation ($R_L = 0.35\ \Omega$), where $I(L_1)$ (current in L_1) is continuous. Figure 10.37 is for discontinuous-mode operation ($R_L = 10\ \Omega$), where $I(L_1)$ becomes discontinuous due to an increased value of R_L . These waveforms are considered to be acceptable.

The design considerations of diode rectifier circuits in high-frequency converters will be discussed later in Subsection 10.6.3.

10.6.2 Flyback Rectifier Diode and Clamping Diode in a Flyback Converter

10.6.2.1 Ideal Circuit

Figure 10.38 shows the basic circuit of a flyback converter. Due to its simple circuit, this type of converter is widely used in low-cost low-power applications. Discontinuous-mode operation (meaning that the magnetizing current in the transformer falls to zero before the end of each switching cycle) is often used because it offers the advantages of easy control and low diode reverse-recovery loss. Figure 10.39 shows the idealized steady-state waveforms for discontinuous-mode operation. These waveforms are obtained from PSpice simulations, based on

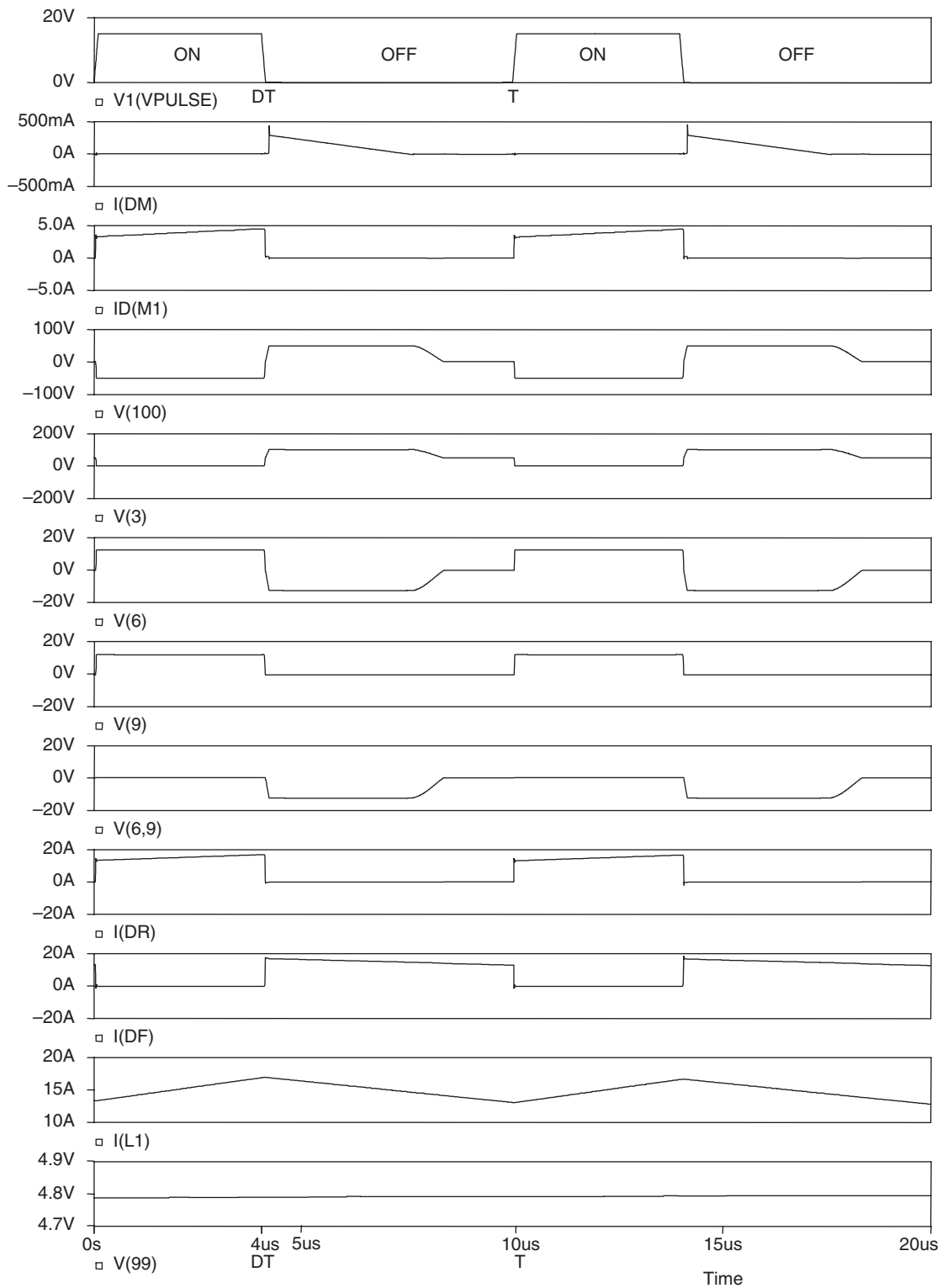


FIGURE 10.31 Waveforms of forward converter using Schottky (fast-speed) diodes as output rectifiers.

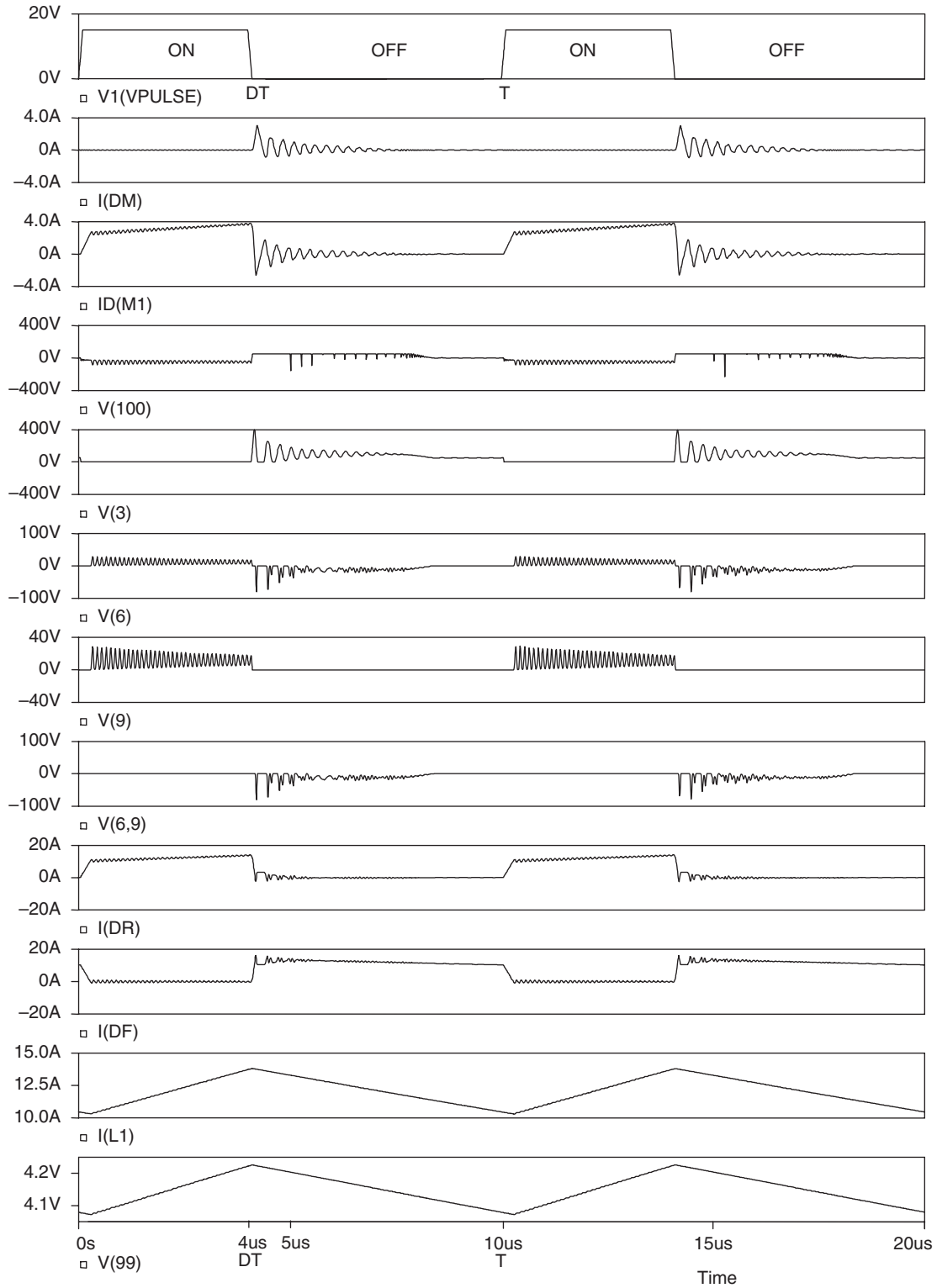


FIGURE 10.32 Waveforms of forward converter with practical transformer and output filtering capacitor having non-zero series effective resistance.

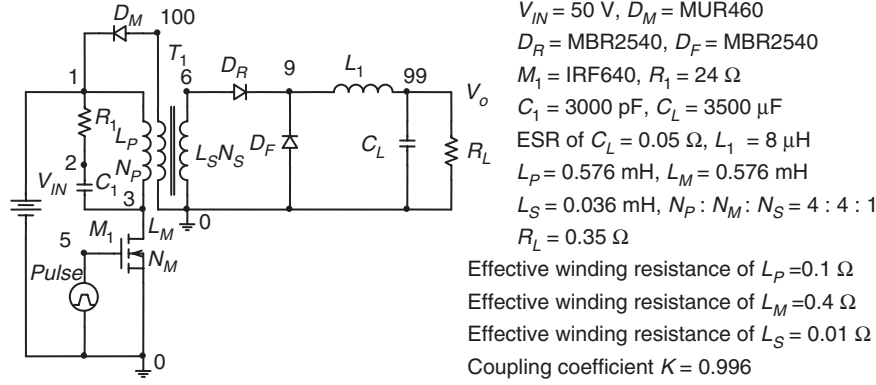


FIGURE 10.33 Forward converter with snubber circuit ($R_1 C_1$) across transformer.

the following assumptions:

- D_R is an idealized rectifier diode with infinitely fast switching speed.
- M_1 is an idealized MOS switch with infinitely fast switching speed and

$$\text{On-state resistance} = 0.067 \Omega$$

$$\text{Off-state resistance} = 1 \text{ M}\Omega$$

- Transformer T_1 has a coupling coefficient of 0.99999999.
- The switching operation of the converter has reached a steady state.

Referring to the circuit shown in Fig. 10.38 and the waveforms shown in Fig. 10.39, the operation of the converter can be explained as follows:

1. For $0 < t < DT$

The switch M_1 is turned on at $t = 0$.

$$V(3) = 0 \quad \text{for } 0 < t < DT$$

The current in M_1 , denoted as $I_D(M_1)$, increases at the rate of

$$\frac{dI_D(M_1)}{dt} = \frac{V_{IN}}{L_P} \quad (10.99)$$

The output rectifier D_R is reversely biased.

2. For $DT < t < (D + D_2)T$

The switching M_1 is turned off at $t = DT$.

The collapse of magnetic flux induces a back emf in L_S to turn-on the output rectifier D_R . The initial amplitude of the rectifier current $I(DR)$, which is also denoted as $I(LS)$, can be found by equating the energy stored in the primary-winding current $I(LP)$ just before

$t = DT$ to the energy stored in the secondary-winding current $I(LS)$ just after $t = DT$:

$$\frac{1}{2} L_P [I(LP)]^2 = \frac{1}{2} L_S [I(LS)]^2 \quad (10.100)$$

$$\frac{1}{2} L_P \left[\frac{V_{IN}}{L_P} DT \right]^2 = \frac{1}{2} L_S [I(LS)]^2 \quad (10.101)$$

$$I(LS) = \sqrt{\frac{L_P}{L_S} \frac{V_{IN}}{L_P} DT} \quad (10.102)$$

$$I(LS) = \frac{N_P}{N_S} \frac{V_{IN}}{L_P} DT \quad (10.103)$$

The amplitude of $I(LS)$ falls at the rate of

$$\frac{dI(LS)}{dt} = \frac{-V_o}{L_S} \quad (10.104)$$

and $I(LS)$ falls to zero at $t = (D + D_2)T$. Since $D_2 V_o = V_{IN} (N_S/N_P) D$

$$D_2 = \frac{V_{IN}}{V_o} \frac{N_S}{N_P} D \quad (10.105)$$

D_2 is effectively the duty cycle of the output rectifier D_R .

3. For $(D + D_2)T < t < T$

The output rectifier D_R is off.

The output capacitor C_L provides the output current to the load R_L .

The switching cycle restarts when the switch M_1 is turned on again at $t = T$.

From the waveforms shown in Fig. 10.39, the following information (for discontinuous-mode operation)

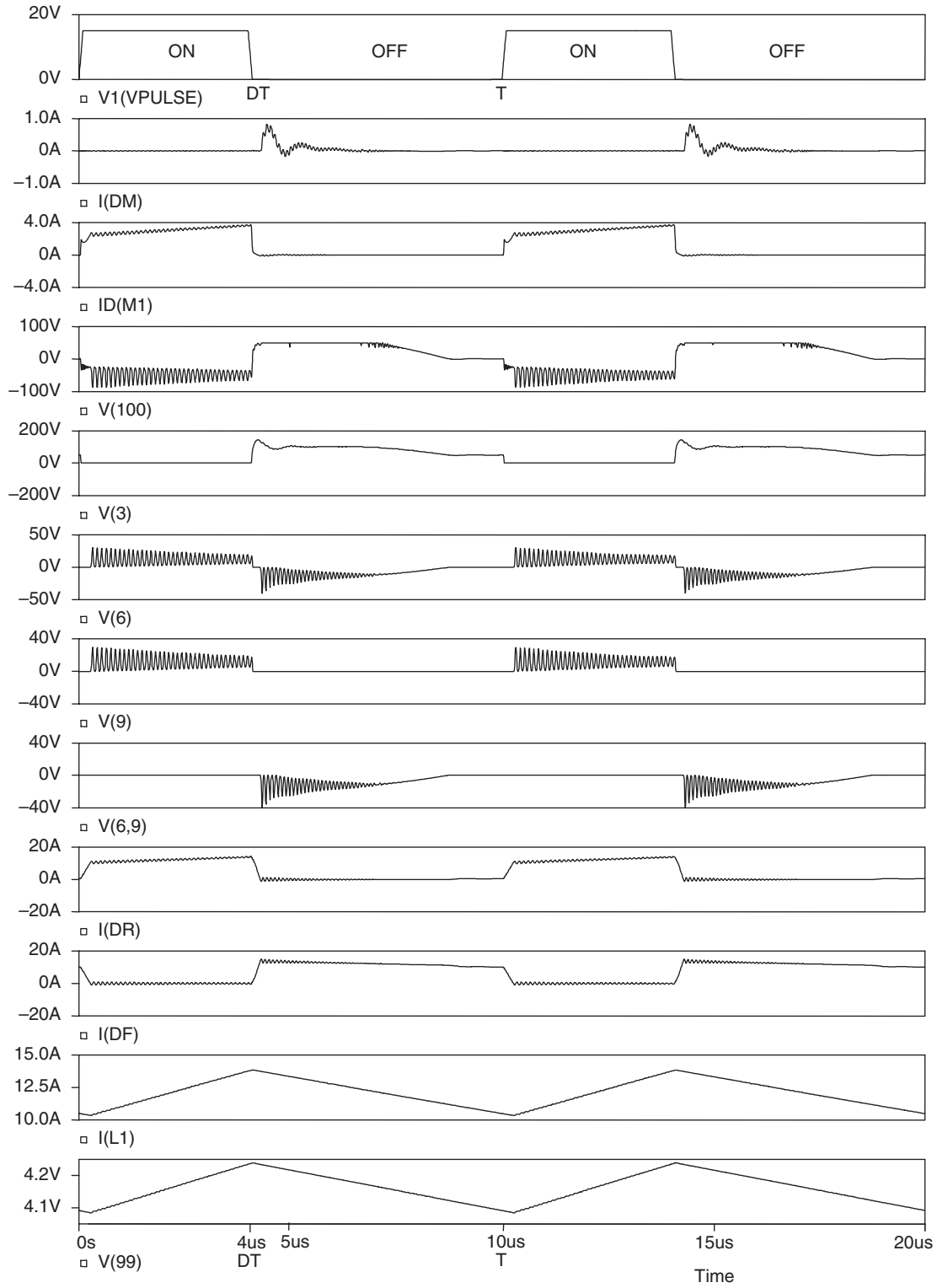


FIGURE 10.34 Waveforms of forward converter with snubber circuit across the transformer.

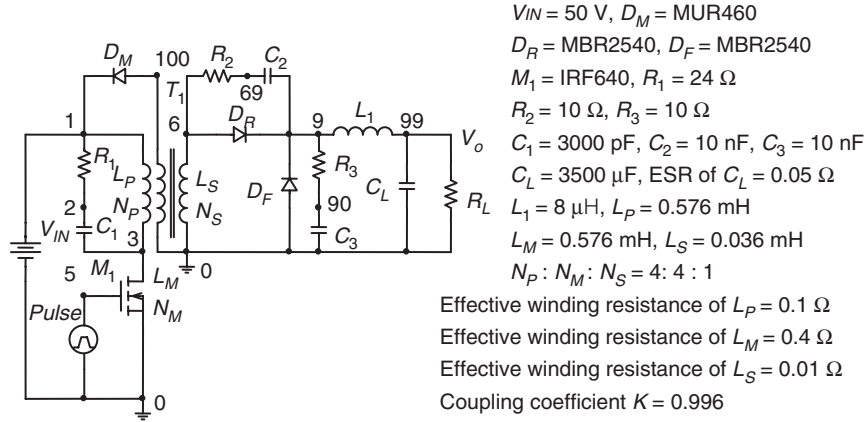


FIGURE 10.35 Practical forward converter with snubber circuits across the transformer and rectifiers.

can be obtained:

- The maximum value of the current in the switch M_1 is

$$ID(M1)_{max} = \frac{V_{IN}}{L_P} DT \quad (10.106)$$

- The maximum value of the current in the output rectifier D_R is

$$I(DR)_{max} = \frac{N_P}{N_S} \frac{V_{IN}}{L_P} DT \quad (10.107)$$

- The output voltage V_o can be found by equating the input energy to the output energy within a switching cycle.

$$V_{IN} \times [\text{Charge taken from } V_{IN} \text{ in a switching cycle}] = \frac{V_o^2}{R_L} T$$

$$V_{IN} \left[\frac{1}{2} DT \frac{DT}{L_P} V_{IN} \right] = \frac{V_o^2}{R_L} T \quad (10.108)$$

$$V_o = \sqrt{\frac{R_L T}{2 L_P}} D V_{IN} \quad (10.109)$$

- The maximum reverse voltage of D_R , $V(6,9)$ (which is the voltage at node 6 with respect to node 9), is

$$V(DR)_{max} = V(6,9)_{max} = V_{IN} \frac{N_S}{N_P} + V_o \quad (10.110)$$

10.6.2.2 Practical Circuit

When a practical transformer (with leakage inductance) is used in the flyback converter circuit shown in Fig. 10.38, there will be large ringings. In order to reduce these ringings to practically acceptable levels, snubber and clamping circuits have to be added. Figure 10.40 shows a practical flyback converter circuit where a resistor–capacitor snubber ($R_2 C_2$) is used to

damp the ringing voltage across the output rectifier D_R , and a resistor–capacitor–diode clamping ($R_1 C_1 D_S$) is used to clamp the ringing voltage across the switch M_1 . What the diode D_S does here is to allow the energy stored by the current in the leakage inductance to be converted to the form of a dc voltage across the clamping capacitor C_1 . The energy transferred to C_1 is then dissipated slowly in the parallel resistor R_1 , without ringing problems.

The simulated waveforms of the flyback converter (circuit given in Fig. 10.40) for discontinuous-mode operation are shown in Fig. 10.41, where the following assumptions are made:

- D_R and D_S are MUR460 ultra-fast diodes.
- M_1 is an IRF640 MOS transistor.
- Transformer T_1 has a practical coupling coefficient of 0.992.
- The effective winding resistance of L_P is 0.025 Ω . The effective winding resistance of L_S is 0.1 Ω .
- The effective series resistance of the output filtering capacitor C_L is 0.05 Ω .
- The switching operation of the converter has reached a steady state.

The waveforms shown in Fig. 10.40 are considered to be acceptable.

10.6.3 Design Considerations

In the design of rectifier circuits, it is necessary for the designer to determine the voltage and current ratings of the diodes. The idealized waveforms and expressions for the maximum diode voltages and currents given under the heading of “Ideal circuit” above (for both forward and flyback converters) are a good starting point. However, when parasitic/stray components are also considered, the simulation results given under

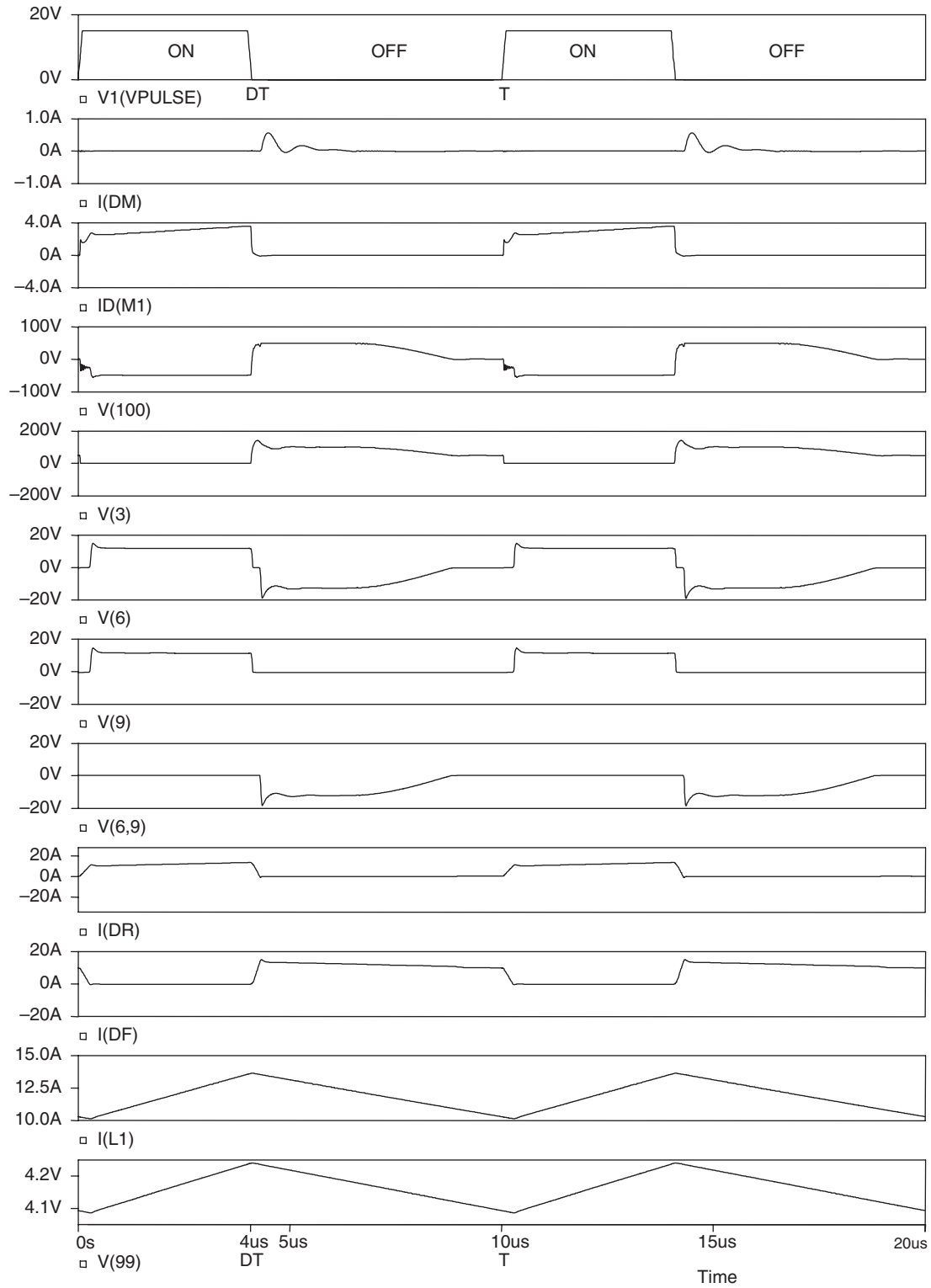


FIGURE 10.36 Waveforms of practical forward converter for continuous-mode operation.

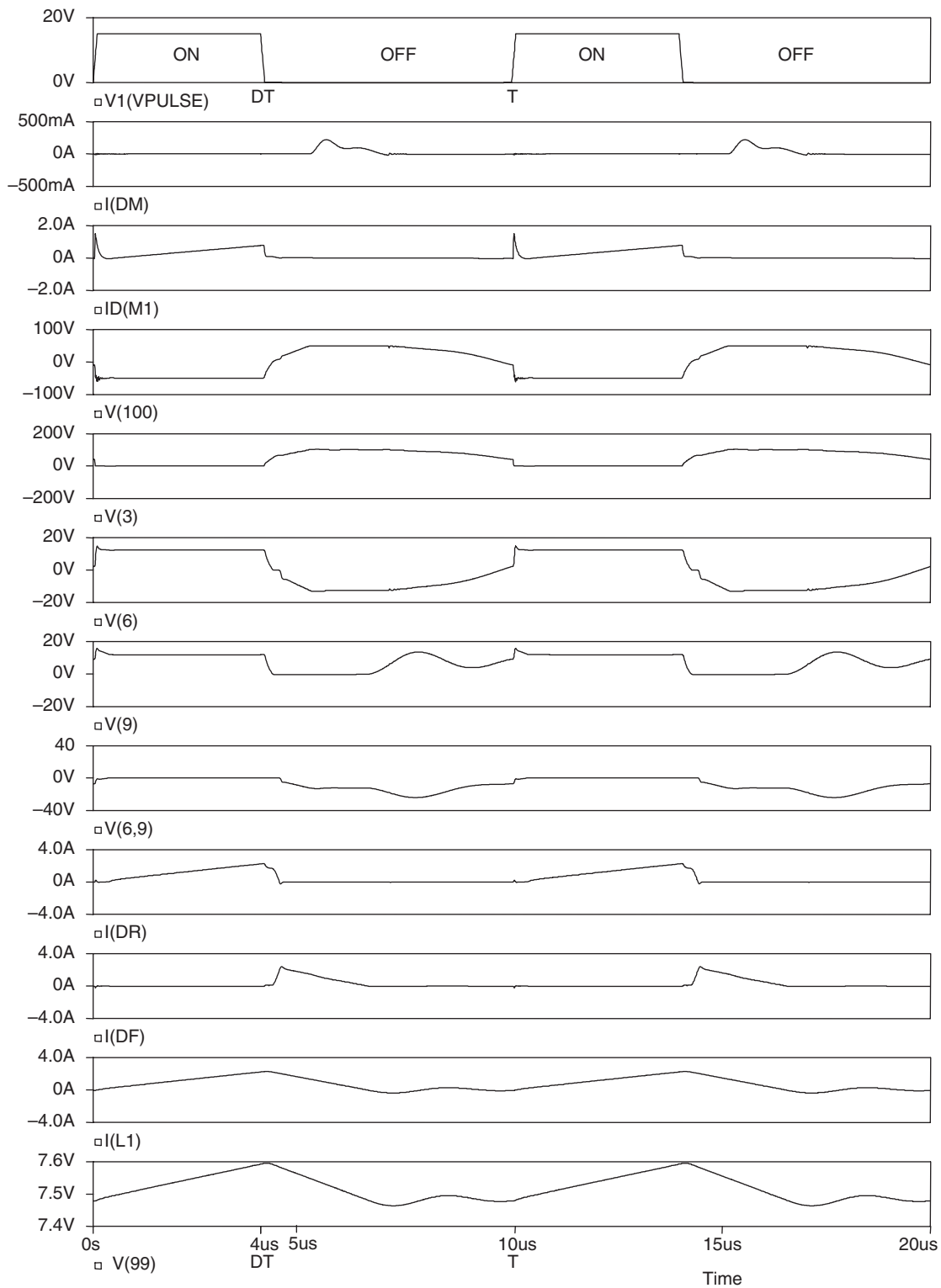


FIGURE 10.37 Waveforms of practical forward converter for discontinuous-mode operation.

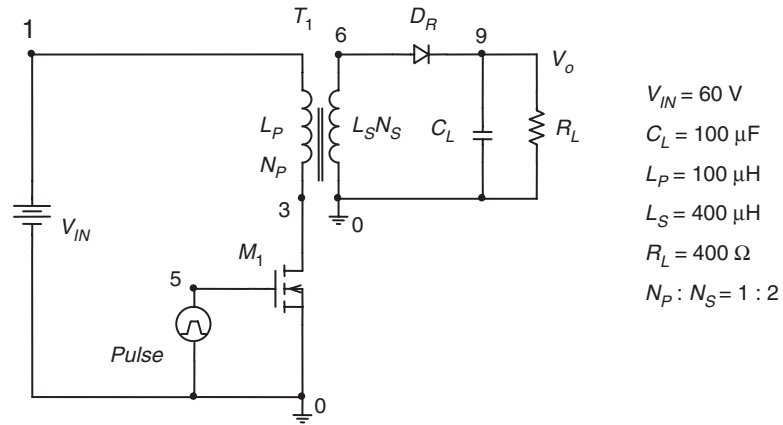


FIGURE 10.38 Basic circuit of flyback converter.

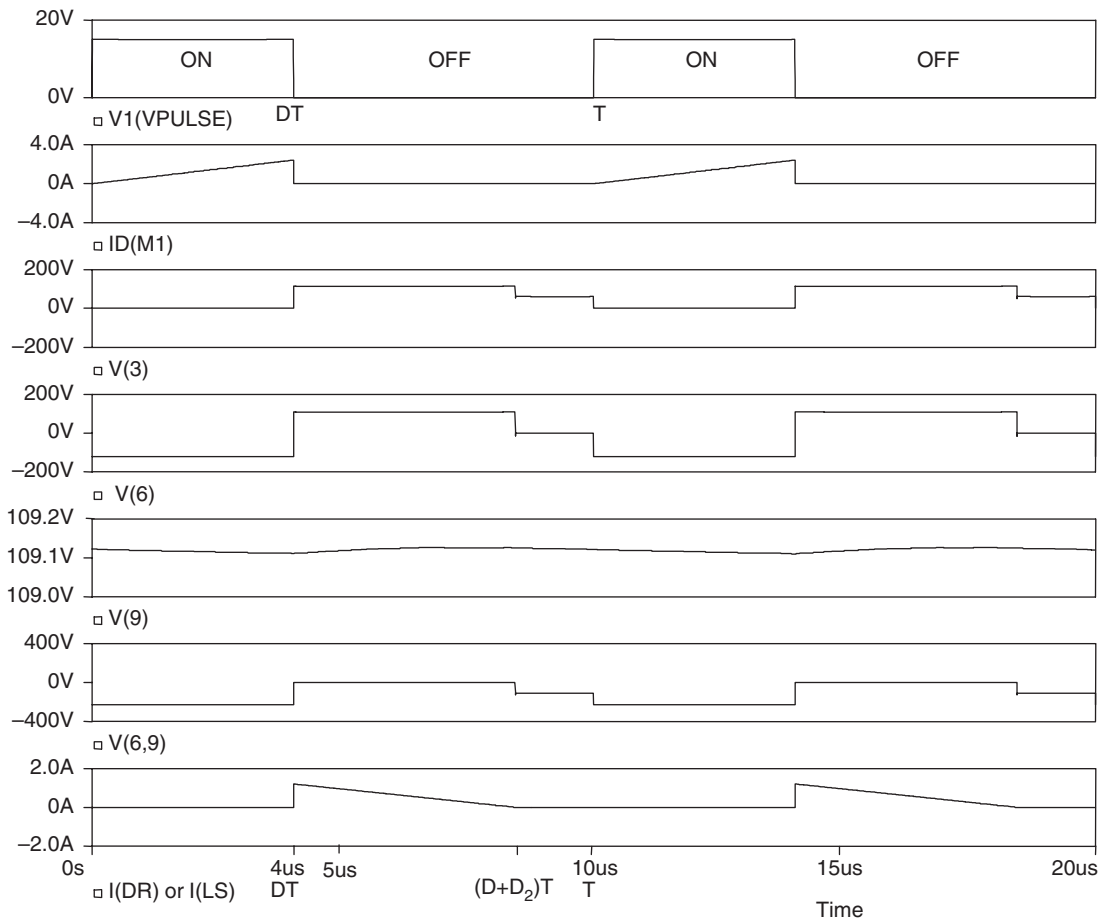


FIGURE 10.39 Idealized steady-state waveforms of flyback converter for discontinuous-mode operation.

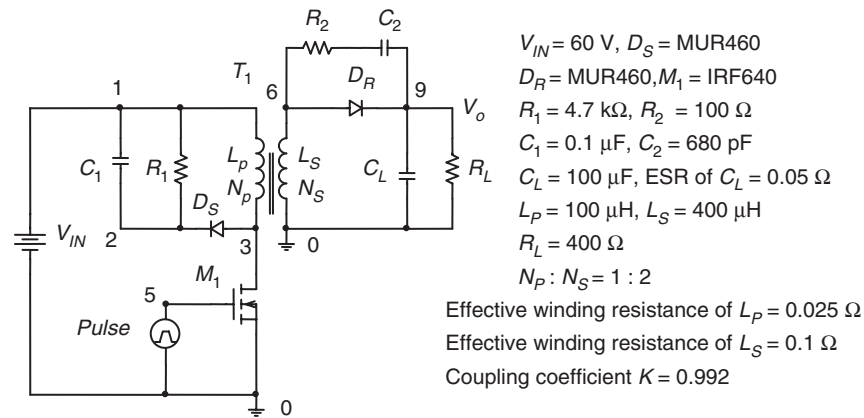


FIGURE 10.40 Practical flyback converter circuit.

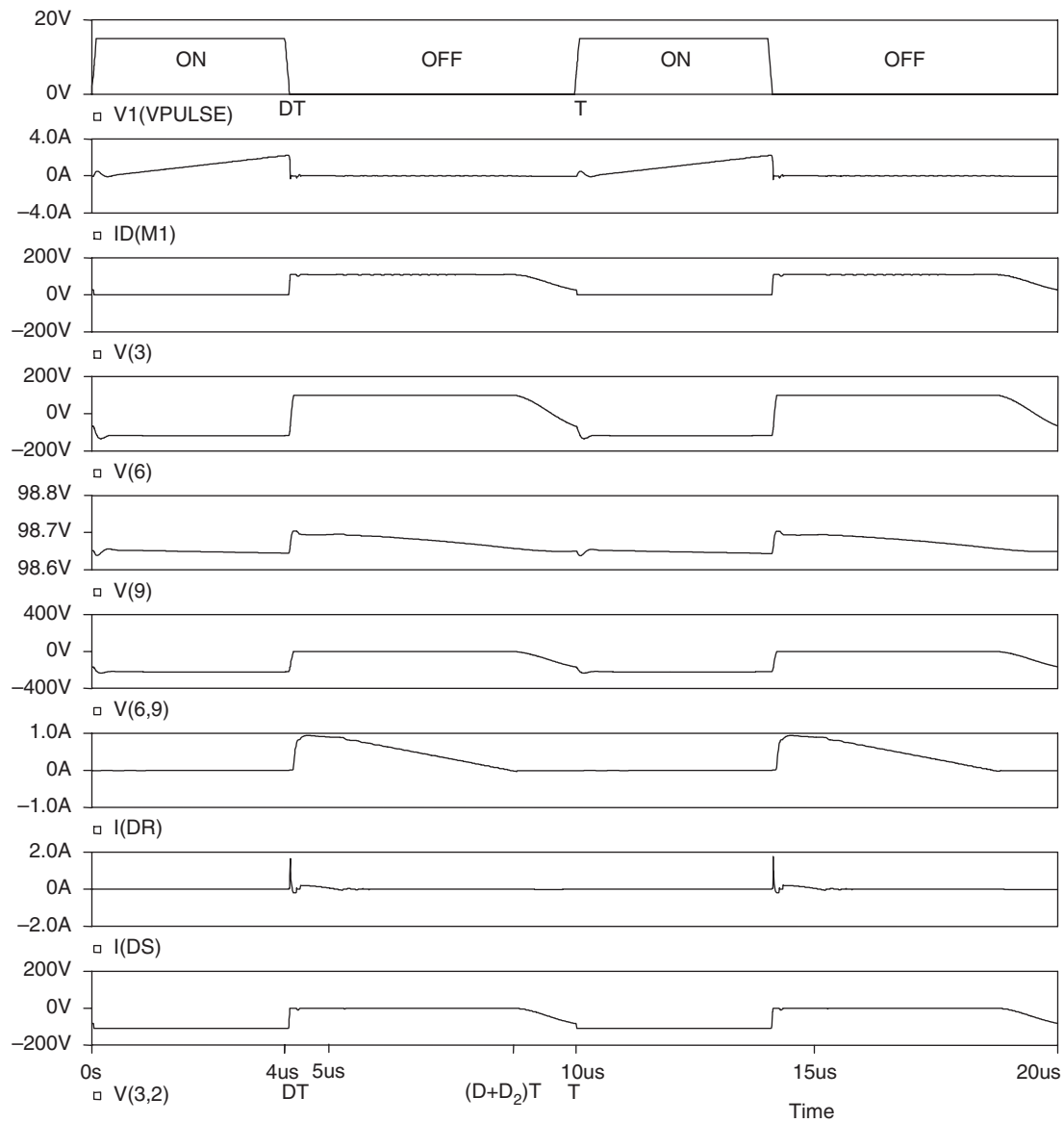


FIGURE 10.41 Waveforms of practical flyback converter for discontinuous-mode operation.

“Practical circuit” are much more useful for the determination of the voltage and current ratings of the high-frequency rectifier diodes.

Assuming that the voltage and current ratings have been determined, proper diodes can be selected to meet the requirements. The following are some general guidelines on the selection of diodes:

- For low-voltage applications, Schottky diodes should be used because they have very fast switching speed and low forward voltage drop. If Schottky diodes cannot be used, either because of their low reverse breakdown voltage or because of their large leakage current (when reversely biased), ultra-fast diodes should be used.
- The reverse breakdown-voltage rating of the diode should be reasonably higher (e.g. 10 or 20% higher) than the maximum reverse voltage, the diode is expected to encounter under the worst-case condition. However, an overly-conservative design (using a diode with much higher breakdown voltage than necessary) would result in a lower rectifier efficiency, because a diode having a higher reverse-voltage rating would normally have a larger voltage drop when it is conducting.
- The current rating of the diode should be substantially higher than the maximum current the diode is expected to carry during normal operation. Using a diode with a relatively large current rating has the following advantages:
 - It reduces the possibility of damage due to transients caused by start-up, accidental short circuit, or random turning on and off of the converter.
 - It reduces the forward voltage drop because the diode is operated in the lower current region of the V – I characteristic.

In some of the “high-efficiency” converter circuits, the current rating of the output rectifier can be many times larger than the actual current expected in the rectifier. In this way, a higher efficiency is achieved at the expense of a larger silicon area.

In the design of R – C snubber circuits for rectifiers, it should be understood that a larger C (and a smaller R) will give

better damping. However, a large C (and a small R) will result in a large switching loss (which is equal to $0.5CV^2f$). As a guideline, a capacitor with five to ten times the junction capacitance of the rectifier may be used as a starting point for iterations. The value of the resistor should be chosen to provide a slightly underdamped operating condition.

10.6.4 Precautions in Interpreting Simulation Results

In using the simulated waveforms as references for design purposes, attention should be paid to the following:

- The voltage/current spikes that appear in the practically measured waveforms may not appear in the simulated waveforms. This is due to the lack of a model in the computer simulation to simulate unwanted coupling among the practical components.
- Most of the computer models of diodes, including those used in the simulations given above, do not take into account the effects of the forward recovery time. (The forward recovery time is not even mentioned in most manufacturers’ data sheets.) However, it is also interesting to note that in most cases the effect of the forward recovery time of a diode is masked by that of the effective inductance in series with the diode (e.g. the leakage inductance of a transformer).

Further Reading

1. *Rectifier Applications Handbook*, 3rd ed., Phoenix, Ariz.: Motorola, Inc., 1993.
2. M. H. Rashid, *Power Electronics: Circuits, Devices, and Applications*, 2nd ed., Englewood Cliffs, NJ: Prentice Hall, Inc., 1993.
3. Y.-S. Lee, *Computer-Aided Analysis and Design of Switch-Mode Power Supplies*, New York: Marcel Dekker, Inc., 1993.
4. J. W. Nilsson, *Introduction to PSpice Manual, Electric Circuits Using OrCAD Release 9.1*, 4th ed., Upper Saddle River, NJ: Prentice Hall, Inc., 2000.
5. J. Keown, *OrCAD PSpice and Circuit Analysis*, 4th ed., Upper Saddle River, NJ: Prentice Hall, Inc., 2001.